SUPPORTING INFORMATION

RAFT Step-Growth Polymerization of Bis-Acrylamides and their Facile Degradation

Parker T. Boeck[1,2], Joji Tanaka[3], Wei You[3]*, Brent S. Sumerlin[1]*, Adam S. Veige[1,2]*

[1]George & Josephine Butler Polymer Research Laboratory, Center for Macromolecular Sciences & Engineering, Department of Chemistry, United States of Florida, P.O. Box 117200, Gainesville, Florida 32611, United States. Email: sumerlin@chem.ufl.edu

[2]Center for Catalysis, Department of Chemistry, University of Florida, P.O. Box 117200, Gainesville, Florida 32611, United States. Email: veige@chem.ufl.edu

[3]Department of Chemistry, University of North Carolina at Chapel Hill, Chapel Hill, NC, 27599-3290 United States. Email: wyou@unc.edu

Table of Contents

EXPERIMENTAL

1. General Considerations

Materials:

The following chemicals were obtained from commercial sources and used without further purification unless otherwise noted: ethanolamine (Sigma Aldrich, >98%), *N*,*N*'-ethylenebis(acrylamide) (1P Chem, 98%), *N*,*N*'-cystaminebis(acrylamide) (TCI Chemical, >95%), *N*,*N*'-piperazinebis(acrylamide) (TCI Chemical, >98%), *m*-cresol (Thermo Fisher, 99%), tri-*n*-butylphosphine (Sigma Aldrich, 99%), methanol (Fisher Chemical, >99.8%), chloroform-*d* (Cambridge Isotope Laboratories) and dimethylsulfoxide-*d* (Cambridge Isotope Laboratories). Dioxane (Acros Organics, 99.5% extra dry) and *N*,*N*-dimethylacrylamide (Sigma Aldrich, 99%) were passed through a short column of basic alumina prior to use. AIBN (Sigma Aldrich, 99.5%) was recrystallized twice in methanol. Hexane diol was recrystallized from ethyl acetate and stored in a desiccator prior to use. *N*,*N*'-methylenebis(acrylamide) (A2B Chem, 97%) was hot-filtered and then recrystallized in methanol. 2-(((butylthio)carbonothioyl)thio)-2-methylpropanoic acid (BDMAT) was synthesized according to published procedures[1] and recrystallized three times in hexane. Hexane-1,6-diylbis(2-(((butylthio)carbonothioyl)thio)-2-methylpropanoate (CTA_2) was synthesized according to published procedures[1] and azeotroped with acetone three times to remove residual DCM. Bis-maleimide based backbone P(BM-*alt*-CTA_2) and the corresponding 4-acryoylmorpholine graft copolymer PBM-*alt*-CTA_2-*graft*-P(NAM) were synthesized according to published procedures.[1]

An AIBN stock solution (20 mg/mL) was prepared in the polymerization solvent. This solution was then measured by volume based on the reported density of the solvent. It is important to note that for simplicity, the molar concentration of reacting species is calculated as moles of reactants/total solvent volume (but not that of the whole solution).

Polymer Characterization:

All ^{1}H NMR spectra were obtained on a Varian INOVA 2 spectrometer (500 MHz) or Bruker 400 MHz unless otherwise stated. All ^{13}C NMR spectra were obtained on a Bruker 400 MHz. Chemical shifts were reported in ppm using the solvent as an internal reference $CDCl_3$ = 7.26 and DMSO-d_6 = 2.50. All NMR spectra were processed in Mestrenova. Data is reported as follows: chemical shift, multiplicity (s= singlet, d = doublet, t = triplet, q = quartet, dd = doublet of doublets, m = multiplet, b = broad, bm = broad multiplet), and integration.

Conventional gel permeation chromatography analysis (GPC) was performed in *N*,*N*-dimethylacetamide (DMAc with 50 mM LiCl) at 50 °C with a flowrate of 1.0 mL/min and 100 µL

injection volume (Agilent isocratic pump, degasser, and autosampler; ViscoGel Iseries 5 µm guard column and two ViscoGel I-series G3078 mixed bed columns with molecular weight ranges 0-20 x 10^3 and 0-100 x 10^4 g/mol). A refractive index detector (Wyatt Optilab T-rEX) operating at 658 nm was used as a concentration detector. Relative molecular weights were obtained through conventional calibration with PMMA standards of molecular weights ranging from 9.88x10^5 to 220 g/mol.

Intrinsic viscosity and absolute molecular weight were measured with an Agilent 1260 Inifinity Series (degasser, isocratic pump, autosampler) and Wyatt Technology detectors (Dawn Helos – II 18 angle MALS detector, Viscostar-II viscometer, Optilab T-rEX differential refractive index detector) equipped with 3x PLGel-Mixed-BLS (linear SEC separation range of molecular weight from 10 M to 500) and 10 µm PLgel guard column, THF (with BHT stabilizer) was used as the mobile phase and the flow rate was set to 1 mL/min. All samples were run with 100 µL injection volume. The dn/dc of the polymer samples in THF were determined using the instrument assuming 100% mass recovery.

Thermogravimetric analyses (TGA) were measured under nitrogen with a TGA 5500 (TA Instruments). Each sample was dried under dynamic vacuum for 24 h and stored in a desiccator prior to analysis. Typically, 5-10 mg of sample was heated at 20 °C/min from 25 to 600 °C.

Differential scanning calorimetry (DSC) thermograms were obtained with a DSC 2500 (TA Instruments). Typically, 5-10 mg of sample was measured and sealed in a pan. The temperature range scanned was -20 °C to 150 °C. Reported data is from the third cycle.

UV-Vis spectra were measured with a Cary 50 spectrophotometer. Typically, 1 mg of sample was dissolved in 15 mL of DMAc and UV-Vis absorbance was measured from 200-1000 nm.

2. Synthetic Procedures

Model RAFT SUMI Reaction

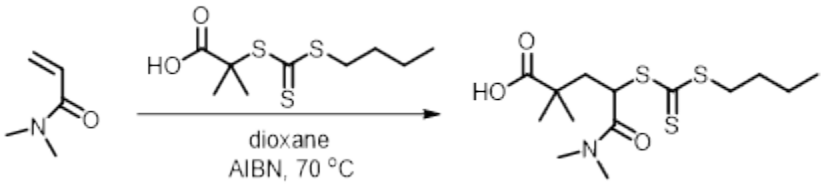

2-(((butylthio)carbonothioyl)thio)-2-methylpropanoic acid (BDMAT) (383.4 mg, 1.52 mmol), dimethylacrylamide (DMA) (150.5 mg, 1.52 mmol), AIBN (6.2 mg, 0.038 mmol), and a stir bar were loaded into a vial. Then, 759 µL of dioxane was added and the mixture was stirred until all solids dissolved. The mixture was then sparged with argon for 10 min. The reaction was then added to an oil bath set to 70 °C. Aliquots were removed intermittently under argon positive pressure for H NMR analysis. DMA conversion was measured via disappearance of the vinyl proton at 5.64 ppm using the CH_3 of BDMAT as an internal standard. CTA consumption was determined via disappearance of the CTA peak at 3.23 ppm using the CH_3 of BDMAT as internal standard. The line fitting tool in Mestrenova was used to determine the peak areas corresponding to the initial CTA at 3.23. Yield of RAFT-SUMI adduct was measured via appearance of the CH bearing the trithiocarbonate using the CH_3 of BDMAT at 0.87 ppm as internal standard.

General $A_2 + B_2$ RAFT Step-Growth Polymerization

[Acrylamide]:[CTA_2]:[AIBN] = 0.5:0.5:0.05. Acrylamide was first added to a vial. Next, CTA_2 was added via 1 mL syringe and measured by weight. The solvent and AIBN stock solution (20 mg/mL in the polymerization solvent) were added to the vial. A stir bar was added, and the vial was sealed with a rubber septum. The solution was then stirred at room temperature until all solids were dissolved. Once homogenous, the solution was sparged with Argon for 15-20 min. The vial was placed in an oil bath at 70 °C for the appropriate period. After heating, the reaction mixture was added dropwise to 40 mL of methanol in a 50 mL centrifuge tube (with intermittent shaking). The precipitate was collected by centrifugation and decanting of the supernatant. To remove residual solvent, the polymer was redissolved in minimal chloroform and precipitated into methanol. The solids were isolated, and residual methanol was removed overnight under dynamic vacuum. (See table S2 for individual yields)

Monomer conversion was measured by ^{1}H NMR spectroscopy via the disappearance of the vinyl proton at ~5.7 ppm relative to the CH_3 at ~0.87 ppm. A single ~25-50 µL aliquot was taken and split for ^{1}H NMR spectroscopy and GPC analysis at each timepoint.

Table S1. Reagent table for RAFT step-growth polymerizations.

Entry	Solvent	Reagent	Amount	Mmol	Isolated Yield (%)
1	*m*-cresol (489 µL)	MBA	63.9 mg	0.414	46.3
		CTA_2	243.3 mg	0.4144	
		AIBN Stock	340 µL		
2	*m*-cresol (566 µL)	EBA	92.5 mg	0.549	39.4
		CTA_2	322.8 mg	0.5499	
		AIBN Stock	452 µL		
3	*m*-cresol (233 µL)	CBA	71.8 mg	0.276	44.6
		CTA_2	161.9 mg	0.2758	
		AIBN Stock	226 µL		
4	dioxane (628 µL)	PBA	103.5 mg	0.5328	44.1
		CTA_2	312.8 mg	0.5329	
		AIBN Stock	438 µL		

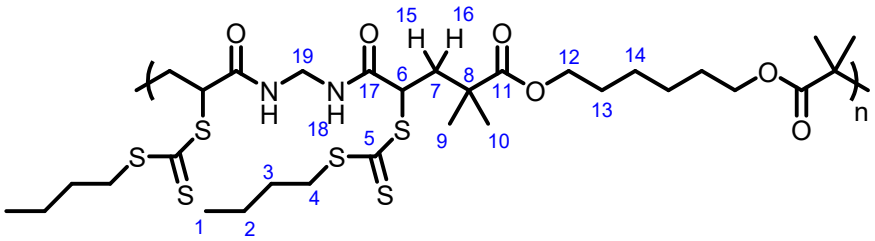

^{1}H and ^{13}C chemical shift assignments (in ppm) for **P(MBA-*alt*-CTA$_2$)**.

^{1}H NMR ($CDCl_3$, 500 MHz) δ (ppm): 7.20 (s, 2H, H_{18}), 4.67 (bm, 2H, H_6), 4.52 (bm, 2H, H_{19}), 4.01 (bm, 4H, H_{12}), 3.33 (bm, 4H, H_4), 2.36 (bm, 2H, H_{15}), 2.05 (bm, 2H, H_{16}), 1.66 (bm, 4H, H_3), 1.60 (bm, 4H, H_{13}), 1.40 (bm, 4H, H_2), 1.34 (bm, 4H, H_{14}), 1.18 (s, 6H, H_9), 1.12 (s, 6H H_{10}), 0.91 (bm, 6H, H_1).

^{13}C NMR ($CDCl_3$, 400 MHz) δ (ppm): 223.18 (C5), 176.88 (C11), 170.96 (C17), 64.92 (C12), 50.43 (C6), 44.26 (C19), 42.14 (C8), 39.96 (C7), 37.44 (C4), 29.93 (C3), 28.51 (C13), 26.31 (C9), 25.76 (C14), 24.50 (C10), 22.19 (C2), 13.69 (C1).

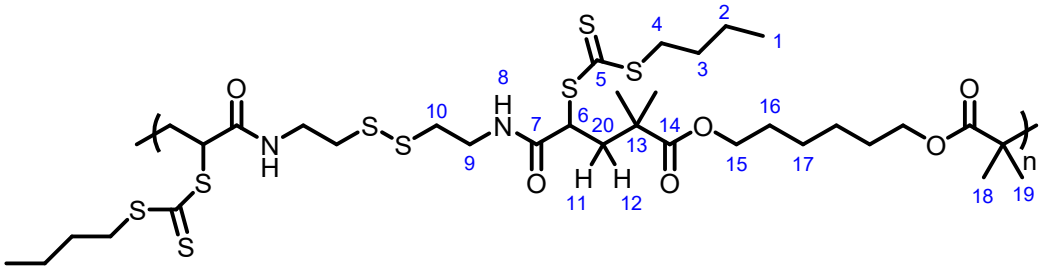

^{1}H and ^{13}C chemical shift assignments (in ppm) for **P(CBA-*alt*-CTA$_2$)**.

^{1}H NMR ($CDCl_3$, 400 MHz) δ (ppm): 6.83 (s, 2H, H_8), 4.75 (t, 2H, *J* = 6.5 Hz, H_6), 4.03 (t, 4H, J = 6.6 Hz, H_{15}), 3.52 (m, 4H, H_9), 3.36 (m, 4H, H_4), 2.73 (t, 4H, 6.4 Hz, H_{10}), 2.45 (dd, 2H, J = 7 Hz and 14.5 Hz, H_{11}), 2.10 (dd, 2H, J = 6 Hz and 14.6 Hz, H_{12}), 1.68 (m, 4H, H_3), 1.63 (m, 4H, H_{16}), 1.43 (m, 4H, H_2), 1.37 (m, 4H, H_{17}), 1.22 (s, 6H, H_{18}), 1.18 (s, 6H, H_{19}), 0.93 (t, 6H, J = 7.4 Hz, H_1).

^{13}C NMR ($CDCl_3$, 400 MHz) δ (ppm): 223.97 (C5), 177.06 (C14), 170.41 (C7), 64.97 (C15), 49.94 (C6), 42.32 (C13), 40.12 (C20), 38.70 (C9), 37.51 (C10), 37.44 (C4), 30.02 (C3), 28.59 (C16), 26.42 (C18), 25.83 (C17), 24.49 (C19), 22.22 (C2), 13.77 (C1).

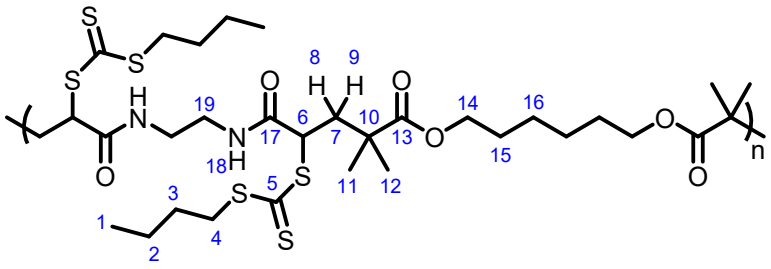

^{1}H and ^{13}C chemical shift assignments (in ppm) for **P(EBA-*alt*-CTA$_2$)**.

^{1}H NMR (DMSO-d_6, 400 MHz) δ (ppm): 8.28 (bs, 2H, H_{18}), 4.64 (m, 2H, H_6), 3.94 (t, 4H, J = 6 Hz, H_{14}), 3.35 (m, 4H, H_4), 3.08 (s, 4H, H_{19}), 2.25 (m, 2H, H_8), 2.00 (m, 2H, H_9), 1.59 (m, 4H, H_3), 1.56 (m, 4H, H_{15}), 1.35 (m, 4H, H_2), 1.32 (m, 4H, H_{16}), 1.13 (s, 12H, $H_{11,12}$), 0.87 (t, 6H, J = 7.5 Hz, H_1).

^{13}C NMR ($CDCl_3$, 400 MHz) δ (ppm): 177.77 (C13), 170.05 (C17), 64.47 (C14), 50.11 (C6), 42.07 (C10), 40.94 (C7), 39.32 (C19), 37.39 (C4), 29.87 (C3), 28.45 (C15), 25.75 (C16), 25.33 (C11), 24.99 (C12), 22.11 (C2), 13.64 (C1).

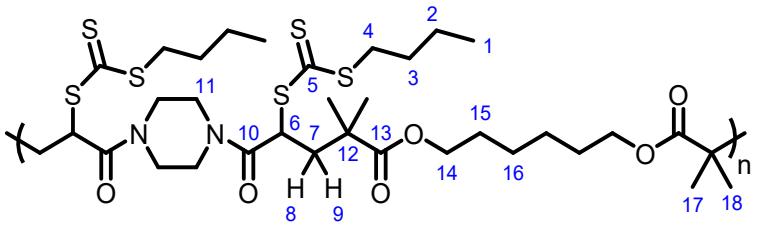

^{1}H and ^{13}C chemical shift assignments (in ppm) for **P(PBA-*alt*-CTA$_2$)**.

^{1}H NMR ($CDCl_3$, 400 MHz) δ (ppm): 5.29 (bm, 2H, H_6), 4.02 (bm, 4H, H_{14}), 3.59 (bm, 6H, H_{11}), 3.35 (bm, 4H, H_4), 2.58 (bm, 2H, H_8), 1.94 (bm, 2H, H_9), 1.67 (bm, 4H, H_3), 1.65 (bm, 4H, H_{15}), 1.43 (bm, 4H, H_2), 1.39 (bm, 4H, H_{16}), 1.22 (bm, 6H, H_{17}), 1.16 (bm, 6H, H_{18}), (0.93 bm, 6H, H_1).

^{13}C NMR ($CDCl_3$, 400 MHz) δ (ppm): 222.37 (C5), 176.87 (C13), 168.52 (C10), 65.01 (C14), 46.46 (C6), 45.77 (C11), 43.09 (C7), 42.35 (C12), 37.37 (C4), 29.98 (C3), 28.56 (C15), 25.89 (C16), 25.75 (C17), 25.40 (C18), 22.18 (C2), 13.72 (C1).

P(CBA-*alt*-CTA$_2$) Degradation

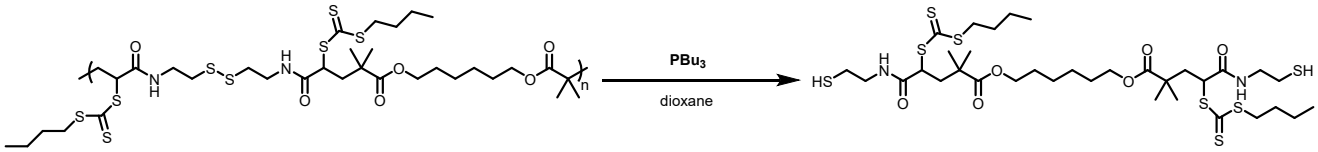

A vial was charged with **P(CBA-*alt*-CTA$_2$)** (24.2 mg, 0.0285mmol), a stir bar, and 600 µL dioxane. The mixture was stirred until full dissolution was achieved. PBu_3 (14.2 µL, 0.0571 mmol) was added via micropipette. After stirring for 5 min, an aliquot was taken, and two drops of water was added to quench PBu_3. The aliquot was then used for GPC analysis.

P(MBA-*alt*-CTA$_2$) Degradation in dioxane

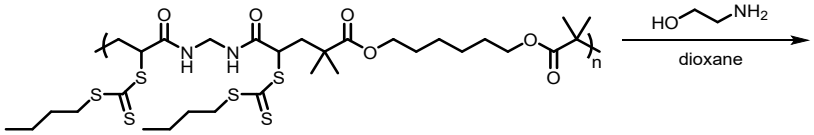

A vial was charged with **P(MBA-*alt*-CTA$_2$)** (10.8 mg, 0.0140 mmol), a stir bar, and dioxane (232 µL). The vial was capped with a rubber septum and the mixture was stirred until the solids were dissolved. Next, ethanolamine (12.7 µL, 0.210 mmol) was added to the vial. The reaction was then allowed to stir for 2 h. After roughly 20 min, the solution became colorless and clear. Then, the solution briefly turned cloudy white before becoming clear again. Aliquots were removed for GPC analysis intermittently. A roughly 20-fold excess of PBu_3 was added, and an aliquot was removed for GPC analysis which was quenched with ~2 drops of water.

P(MBA-*alt*-CTA$_2$) Degradation in $CDCl_3$

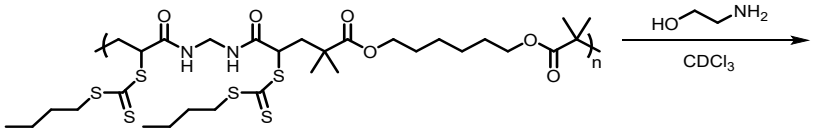

P(MBA-*alt*-CTA$_2$) (37.0 mg, 0.0480 mmol) was dissolved in 794 µL $CDCl_3$, and the solution was transferred to an NMR tube. A ^{1}H NMR was taken, and an aliquot was removed for GPC analysis. Next, excess ethanolamine (43.4 µL, 0.719 mmol) was added via micropipette. The NMR tube was shaken vigorously by hand for 10 min at which point an NMR was taken. The NMR tube was shaken vigorously for 20 min at which point another NMR was taken. The reaction was continually monitored by NMR spectroscopy and GPC.

P(BM-*alt*-CTA$_2$) Degradation

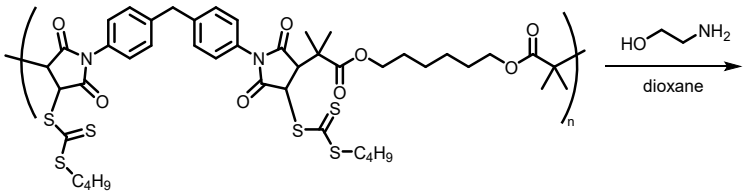

A vial was charged with **P(BM-*alt*-CTA$_2$)** (42.6 mg, 0.0451 mmol) and a stir bar. Then, 1,4-dioxane (914 mL) was added and the reaction was stirred until the polymer dissolved. The solution was sparged for 15 min with argon and degassed ethanolamine (81.4 µL, 1.35 mmol) was added via syringe. Shortly after the addition of ethanolamine solids precipitated out. After 24 h of stirring there were no remaining solids and an aliquot was removed for GPC analysis.

Synthesis of PBM-*alt*-CTA$_2$-*graft*-P(NAM)-SH

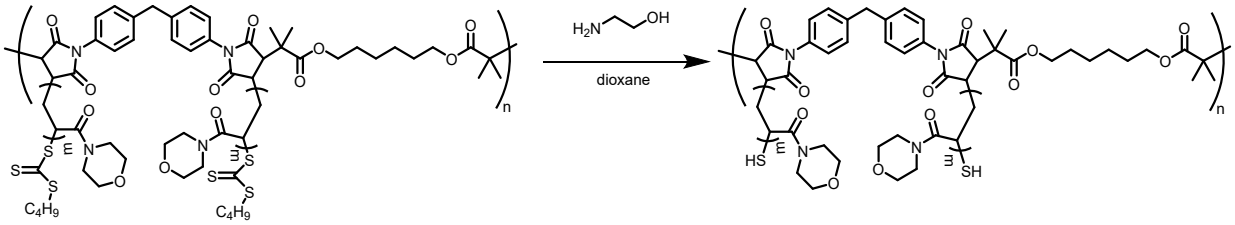

A vial was charged with **PBM-*alt*-CTA$_2$-*graft*-P(NAM)** (54.5 mg, 0.0083 mmol) and a stir bar. Then, dioxane (1.170 mL) was added and the mixture was stirred until all solids dissolved. An aliquot was removed for GPC analysis and then ethanolamine (7.5 µL, 0.13 mmol) was added via micropipette. Aliquots were removed intermittently for GPC analysis. After 20 h the mixture was added dropwise to 40 mL of methanol in a centrifuge tube. The solids were isolated by centrifugation and solvent was removed under reduced pressure overnight yielding **PBM-*alt*-CTA$_2$-*graft*-P(NAM)-SH** in 78.6% yield.

.

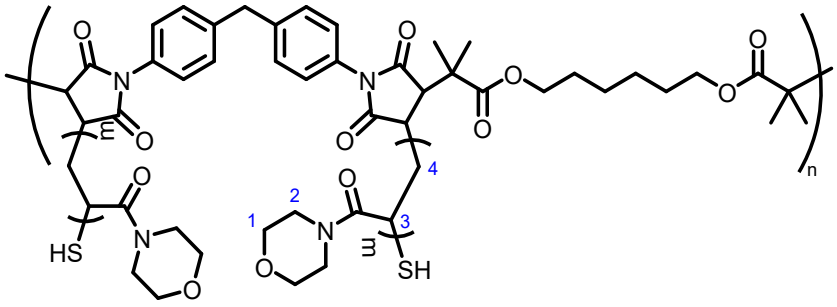

^{1}H NMR ($CDCl_3$, 500 MHz) δ (ppm): 4.11-3.06 (b, 8H, $H_{1,2}$), 2.87-2.22 (b, 1H, H_3), 3.59 (b, 3H, H_4).

3. RAFT SUMI Study Data

Table S2. Kinetic data for model RAFT SUMI reaction

Time (h)	$[M]_t/[M]_0$[a]	$[CTA]_t/[CTA]_0$[b]	Yield% [c]
0	1.00	1.00	0
0.5	0.86	0.87	14
1.0	0.72	0.73	28
2.0	0.44	0.48	51
4.0	0.17	0.22	77
12.0	0.01	0.06	94

[a] DMA conversion was measured via disappearance of the vinyl proton at 5.64 ppm using the CH_3 of BDMAT as internal standard.

[b] CTA consumption was determined via disappearance of the CTA peak at 3.23 ppm using the CH_3 of BDMAT as internal standard.

[c] Yield of RAFT-SUMI adduct was measured via appearance of the CH bearing the trithiocarbonate using the CH_3 of BDMAT at 0.87 ppm as internal standard.

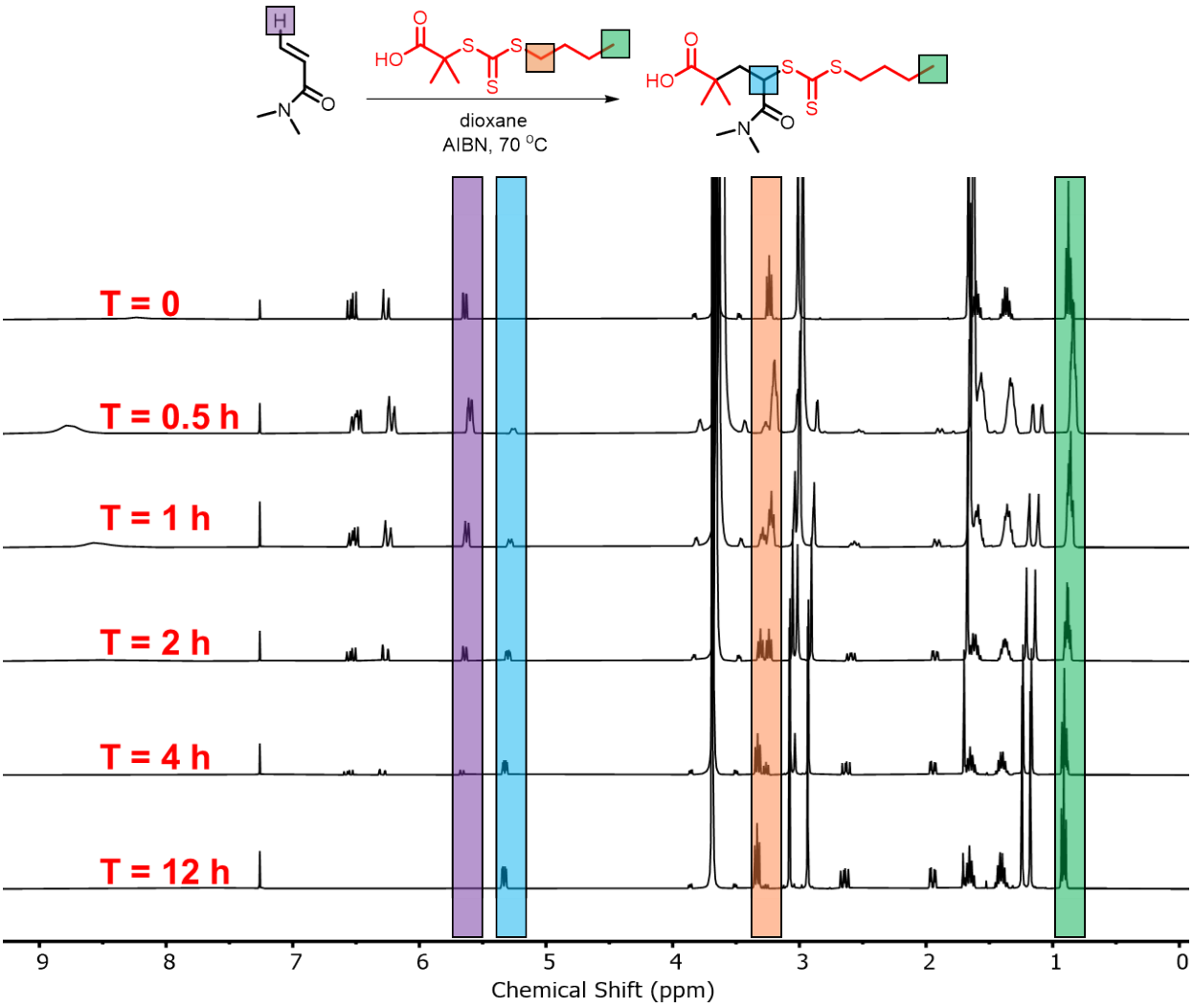

Figure S1. ^{1}H NMR spectra ($CDCl_3$, 400 MHz, 25 °C) used for determining CTA (orange) and DMA (purple) conversion as well as RAFT-SUMI product yield (blue) using the CH_3 of BDMAT (green) as internal standard. **Note that sparging causes evaporation of DMA leading to a slight excess of BDMAT at T = 0.**

4. Equations

Theoretical molecular weight averages used for producing the functions in **Figure 2A-D** were calculated according the following equations which describe the increase of M_n, M_w, and M_z with increasing conversion (p), originally described by Flory.[2]

$$M_n = M_0 \frac{1}{1-p} \quad \text{(Eq. S1)}$$

$$M_w = M_0 \frac{1+p}{1-p} \quad \text{(Eq. S2)}$$

$$M_z = M_0 \frac{1+4p+p^2}{1-p^2} \quad \text{(Eq. S3)}$$

Where M_0 (structural molecular weight) is the average molecular weight of a given bis-acrylamide and CTA_2.

It is important to note that Flory's original equations described above neglect to account for the stoichiometric imbalance caused by irreversible termination of bis-acrylamide caused by AIBN initiation. Additionally, they also neglect cyclization. Finally, they assume equal end group reactivity regardless of polymer molecular weight.

5. Kinetic Study Data (Chromatograms and NMR)

Table S3. Kinetic Data for RAFT Step-Growth of **P(MBA-*alt*-CTA_2)**.

Time (h)	p[a]	r_{th}[b]	$M_{w,th}$[c]	$M_{w,th}(r_{th})$[d]	M_w[e]	M_z[e]	M_n[e]	M_w/M_n[e]
0	0	1.000	371	371	n.d	n.d.	n.d.	n.d.
0.5	0.48	0.992	1.1k	1.1k	845	3.1k	361	1.93
1	0.70	0.984	2.1k	2.1k	1.7k	3.2k	841	1.94
1.5	0.83	0.977	4.0k	3.8k	2.9k	4.2k	1.7k	1.70
2	0.89	0.970	6.4k	5.7k	4.2k	6.2k	2.3k	1.84
3	0.94	0.959	12.0k	9.0k	7.0k	11.6k	2.7k	2.55
4	0.97	0.949	24.3k	13.1k	15.2k	27.9k	6.2k	2.46

[a] Measured by ^{1}H NMR spectroscopy via disappearance of the vinyl peak at ~5.7 ppm.
[b] Instantaneous stoichiometric imbalance resulting from AIBN initiation.[1,3]
[c] Theoretical weight-average molecular weight using Flory's equation for an ideal step-growth polymerization.
[d] Theoretical weight-average molecular weight considering initiator derived imbalanced stoichiometry.[1,3]
[e] Measured by GPC analysis in DMAc at 50 °C with PMMA standards.

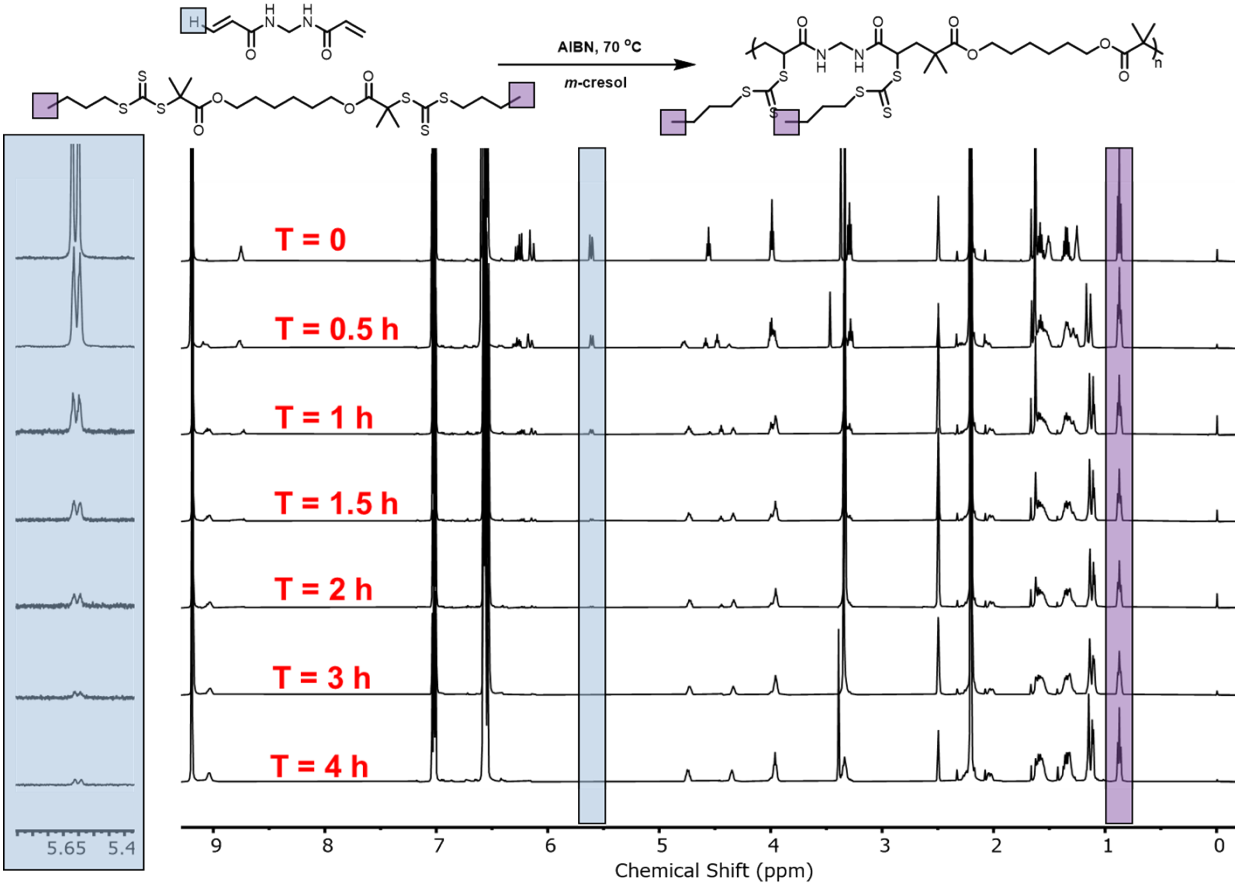

Figure S2. ^{1}H NMR spectra (DMSO-d_6, 500 MHz, 25 °C) used for determination of conversion during RAFT step-growth polymerization of MBA with CTA_2. Conversion was measured via the disappearance of the vinyl peak at ~5.7 ppm (highlighted in blue) using the CH_3 of the Z group (highlighted in purple) as an internal standard.

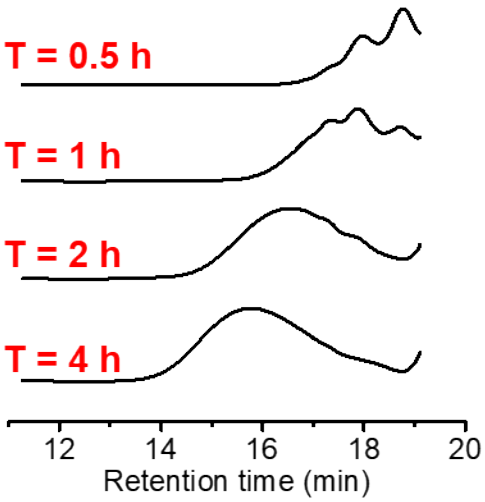

Figure S3. GPC chromatograms (DMAc, 50 °C, dRI detection) showing molecular weight evolution during RAFT-step growth polymerization of MBA and CTA_2 (excluding solvent peak).

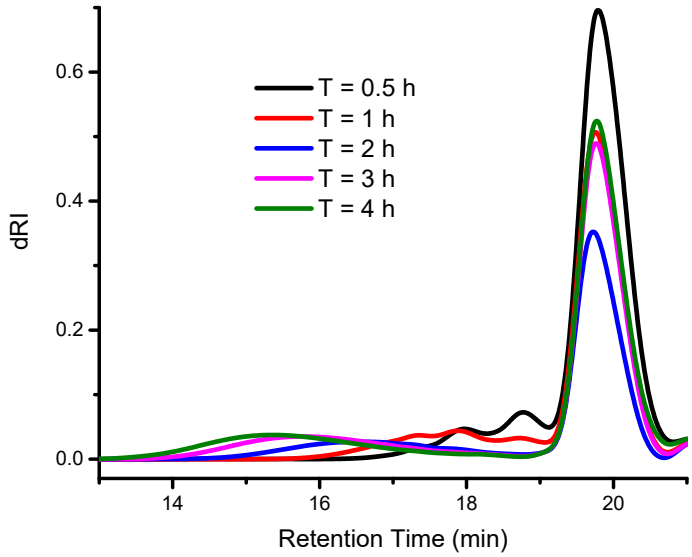

Figure S4. GPC chromatograms (DMAc, 50 °C, dRI detection) showing molecular weight evolution during RAFT-step growth polymerization of MBA and CTA_2 (including solvent peak).

Table S4. Kinetic Data for RAFT Step-Growth of **P(CBA-*alt*-CTA$_2$)**

Entry	Time (h)	p^a	r_{th}^b	$M_{w,th}^c$	$M_{w,th}(r_{th})^d$	M_w^e	M_z^e	M_n^e	M_w/M_n^e
1	0	0	1.000	423	423	n.d	n.d.	n.d.	n.d.
	0.5	0.33	0.992	838	836	1.1k	1.5k	818	1.31
	1	0.55	0.984	1.5k	1.5k	1.7k	2.6k	1.1k	1.56
	2	0.80	0.970	3.9k	3.6k	3.9k	6.4k	1.8k	2.22
	4	0.94	0.949	14.7k	10.2k	10.1k	18.7k	2.5k	3.95
	6	0.98	0.933	32.9k	14.1k	15.6k	33.9k	3.0k	5.24

[a] Measured by ^{1}H NMR spectroscopy via disappearance of the vinyl peak at ~5.6 ppm.
[b] Instantaneous stoichiometric imbalance resulting from AIBN initiation.[1,3]
[c] Theoretical weight-average molecular weight using Flory's equation for an ideal step-growth polymerization.[2]
[d] Theoretical weight-average molecular weight considering initiator derived imbalanced stoichiometry.[1,3]
[e] Measured by GPC analysis in DMAc at 50 °C with PMMA standards.

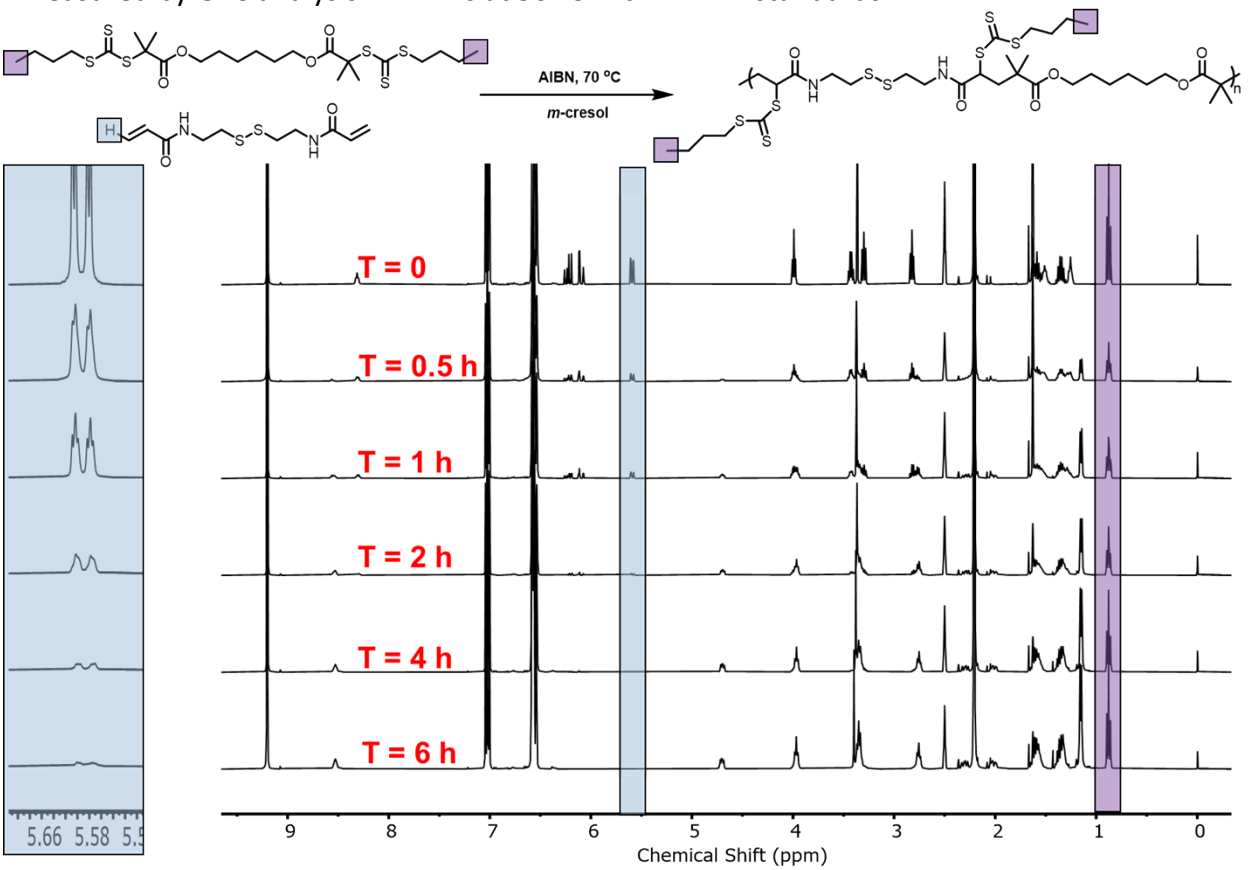

Figure S5. ^{1}H NMR spectra (DMSO-d_6, 400 MHz, 25 °C) used for determination of conversion during RAFT step-growth polymerization of CBA with CTA$_2$. Conversion was measured via the

disappearance of the vinyl peak at ~5.6 ppm (highlighted in blue) using the CH_3 of the Z group (highlighted in purple) as internal standard.

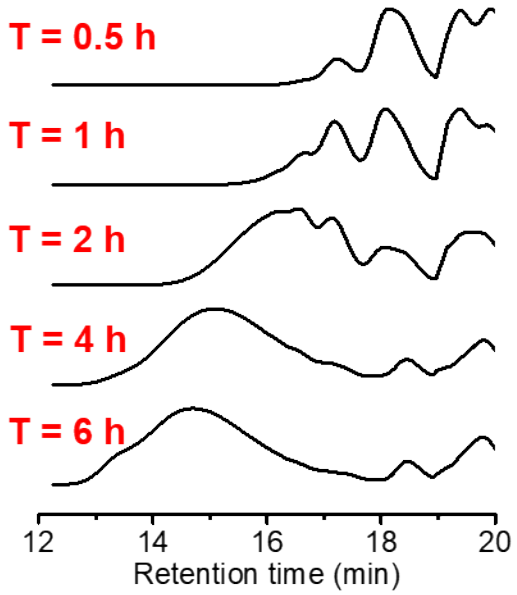

Figure S6. GPC chromatograms (DMAc, 50 °C, dRI detection) showing molecular weight evolution during RAFT step-growth polymerization of CBA and CTA_2 (excluding solvent peak).

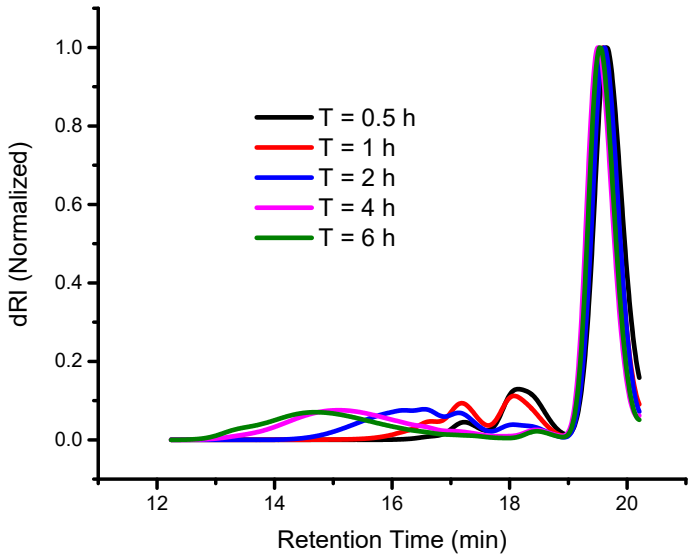

Figure S7. Normalized GPC chromatograms (DMAc, 50 °C, dRI detection) showing molecular weight evolution during RAFT step-growth polymerization of CBA and CTA_2 (including solvent peak).

Table S5. Kinetic Data for RAFT Step-Growth of **P(EBA-*alt*-CTA$_2$)**

Entry	Time (h)	p^a	$r_{th}{}^b$	$M_{w,th}{}^c$	$M_{w,th}(r_{th})^d$	$M_w{}^e$	$M_z{}^e$	$M_n{}^e$	$M_w/M_n{}^e$
1	0	0	1.000	378	378	n.d	n.d.	n.d.	n.d.
	0.5	0.35	0.992	784	782	1.2k	1.7k	921	1.31
	1	0.58	0.984	1.7k	1.7k	1.8k	2.7k	1.2k	1.49
	2	0.81	0.970	4.8k	4.4k	3.5k	5.6k	1.9k	1.86
	4	0.96	0.949	18.3k	11.2k	7.8k	13.8k	3.9k	1.99

[a] Measured by ^{1}H NMR spectroscopy via disappearance of the vinyl peak at ~5.7 ppm.
[b] Instantaneous stoichiometric imbalance resulting from AIBN initiation.[1,3]
[c] Theoretical weight-average molecular weight using Flory's equation for an ideal step-growth polymerization.[2]
[d] Theoretical weight-average molecular weight considering initiator derived imbalanced stoichiometry.[1,3]
[e] Measured by GPC analysis in DMAc at 50 °C with PMMA standards.

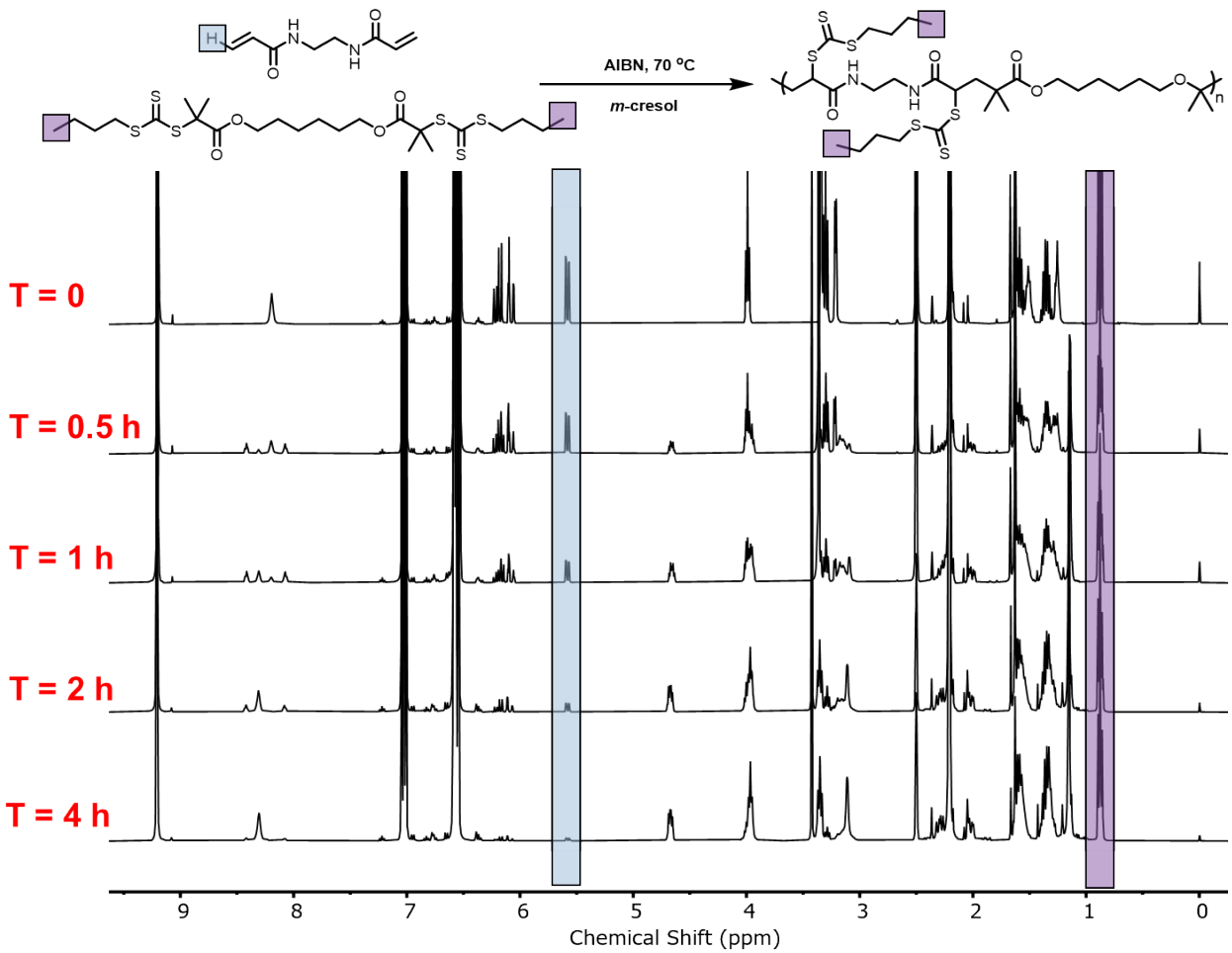

Figure S8. ^{1}H NMR spectra (DMSO-d_6, 400 MHz, 25 °C) used for determination of conversion during RAFT step-growth polymerization of EBA with CTA_2. Conversion was measured via the disappearance of the vinyl peak at ~5.6 ppm (highlighted in blue) using the CH_3 of the Z group (highlighted in purple) as internal standard.

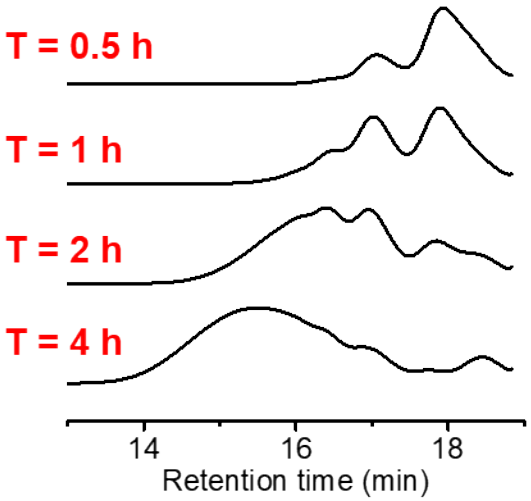

Figure S9. GPC chromatograms (DMAc, 50 °C, dRI detection) showing molecular weight evolution during RAFT step-growth polymerization of EBA and CTA_2.

Table S6. Kinetic Data for RAFT Step-Growth of **P(PBA-*alt*-CTA_2)**

Entry	Time (h)	p^a	r_{th}^b	$M_{w,th}^c$	$M_{w,th}(r_{th})^d$	M_w^e	M_z^e	M_n^e	M_w/M_n^e
1	0	0	1.000	390	390	n.d	n.d.	n.d.	n.d.
	0.5	0.37	0.992	850	848	522	809	350	1.49
	1	0.60	0.984	1.5k	1.5k	976	1.7k	519	1.88
	2	0.84	0.970	4.3k	4.0k	2.9k	4.7k	1.6k	1.81
	4	0.95	0.949	16.2k	10.6k	8.0k	15.5k	3.0k	2.59
	6	0.97	0.933	29.6k	12.9k	13.0k	28.4k	4.2k	3.09
	8	0.98	0.921	48.4k	13.7k	16.7k	38.7k	5.0k	3.31

[a] Measured by ^{1}H NMR spectroscopy via disappearance of the vinyl peak at ~5.7 ppm.
[b] Instantaneous stoichiometric imbalance resulting from AIBN initiation.[1,3]
[c] Theoretical weight-average molecular weight using Flory's equation for an ideal step-growth polymerization.[2]
[d] Theoretical weight-average molecular weight considering initiator derived imbalanced stoichiometry.[1,3]
[e] Measured by GPC analysis in DMAc at 50 °C with PMMA standards.

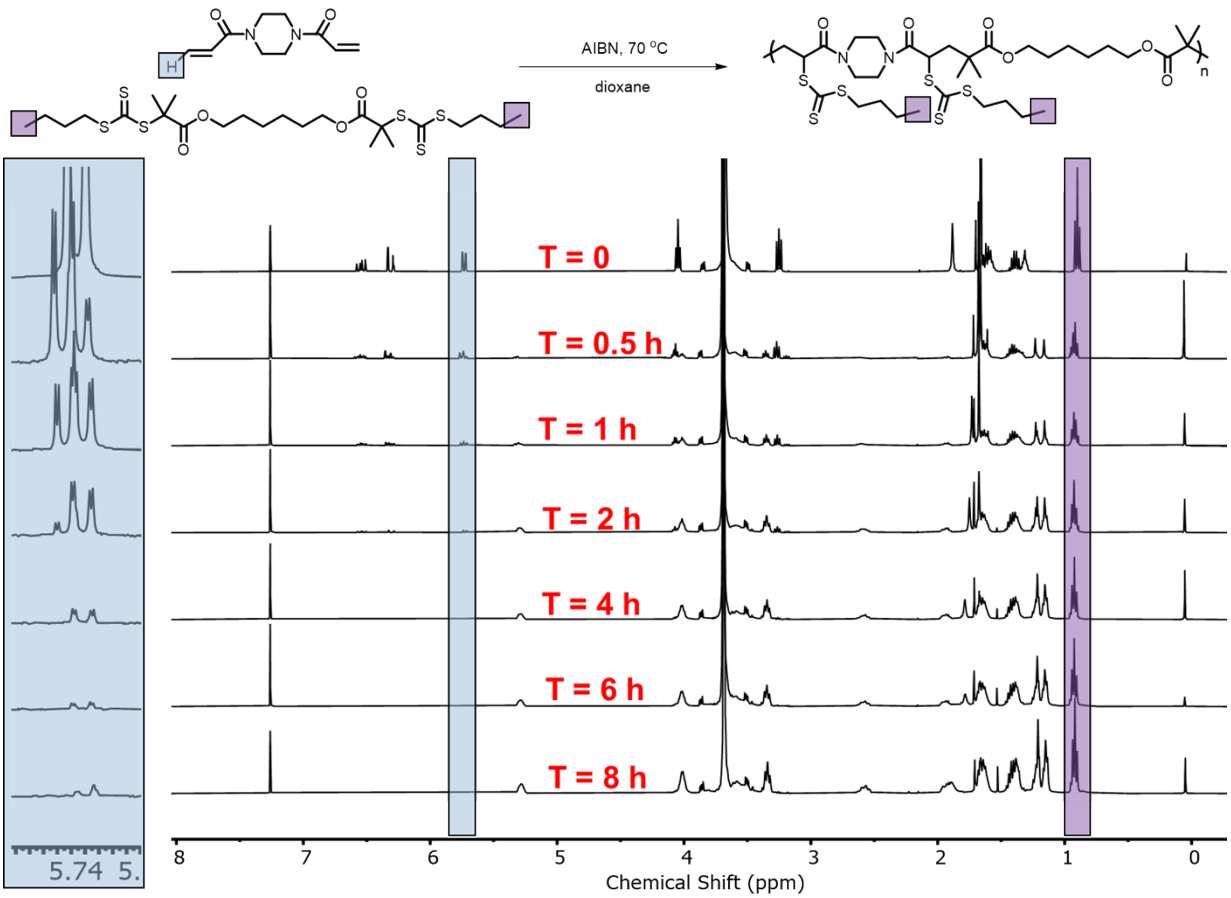

Figure S10. ^{1}H NMR spectra ($CDCl_3$, 400 MHz, 25 °C) used for determination of conversion during RAFT step-growth polymerization of PBA with CTA_2. Conversion was measured via disappearance of the vinyl peak at ~5.7 ppm (highlighted in blue) relative to the CH_3 of the RAFT agent Z group (highlighted in purple).

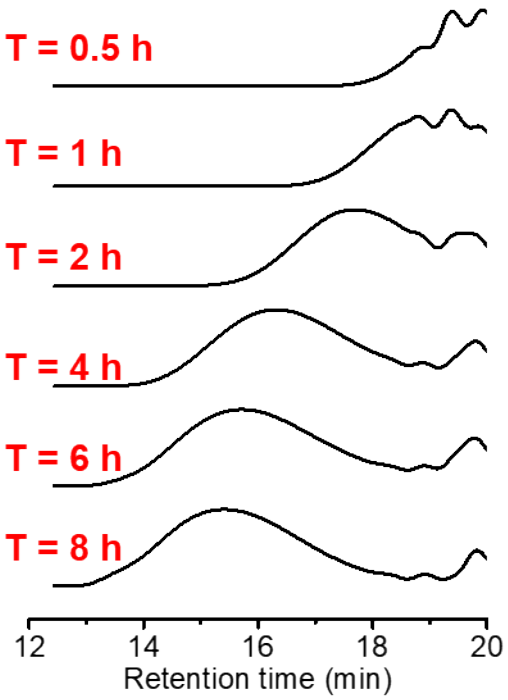

Figure S11. GPC chromatograms (DMAc, 50 °C, dRI detection) showing molecular weight evolution during RAFT step-growth polymerization of PBA and CTA_2. Normalized chromatogram excluding solvent peak.

Note earlier time points had overlap with the solvent peak and may cause overestimation of molecular weight.

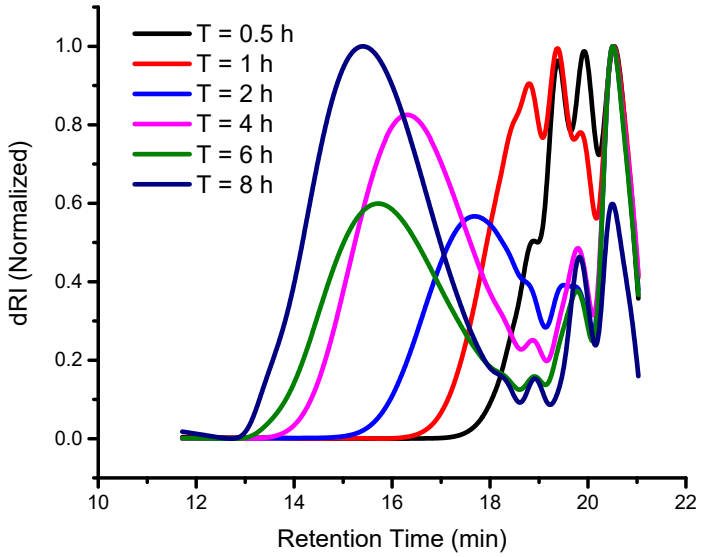

Figure S12. GPC chromatograms (DMAc, 50 °C, dRI detection) showing molecular weight evolution during RAFT step-growth polymerization of PBA and CTA_2 normalized including solvent peak.

6. Isolated Polymer ^{1}H and ^{13}C NMR Spectra

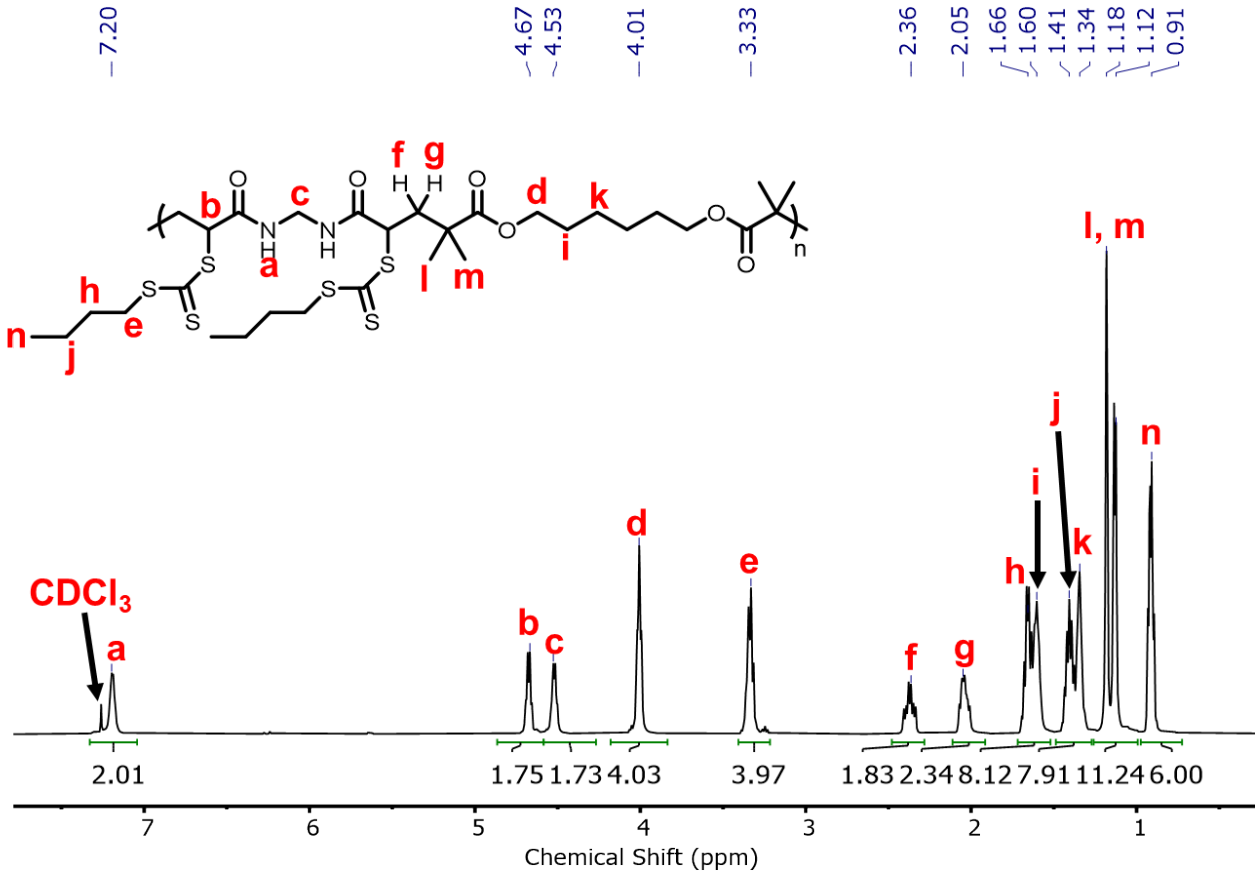

Figure S13. ^{1}H NMR spectrum ($CDCl_3$, 500 MHz, 25 °C) of **P(MBA-*alt*-CTA$_2$)**.

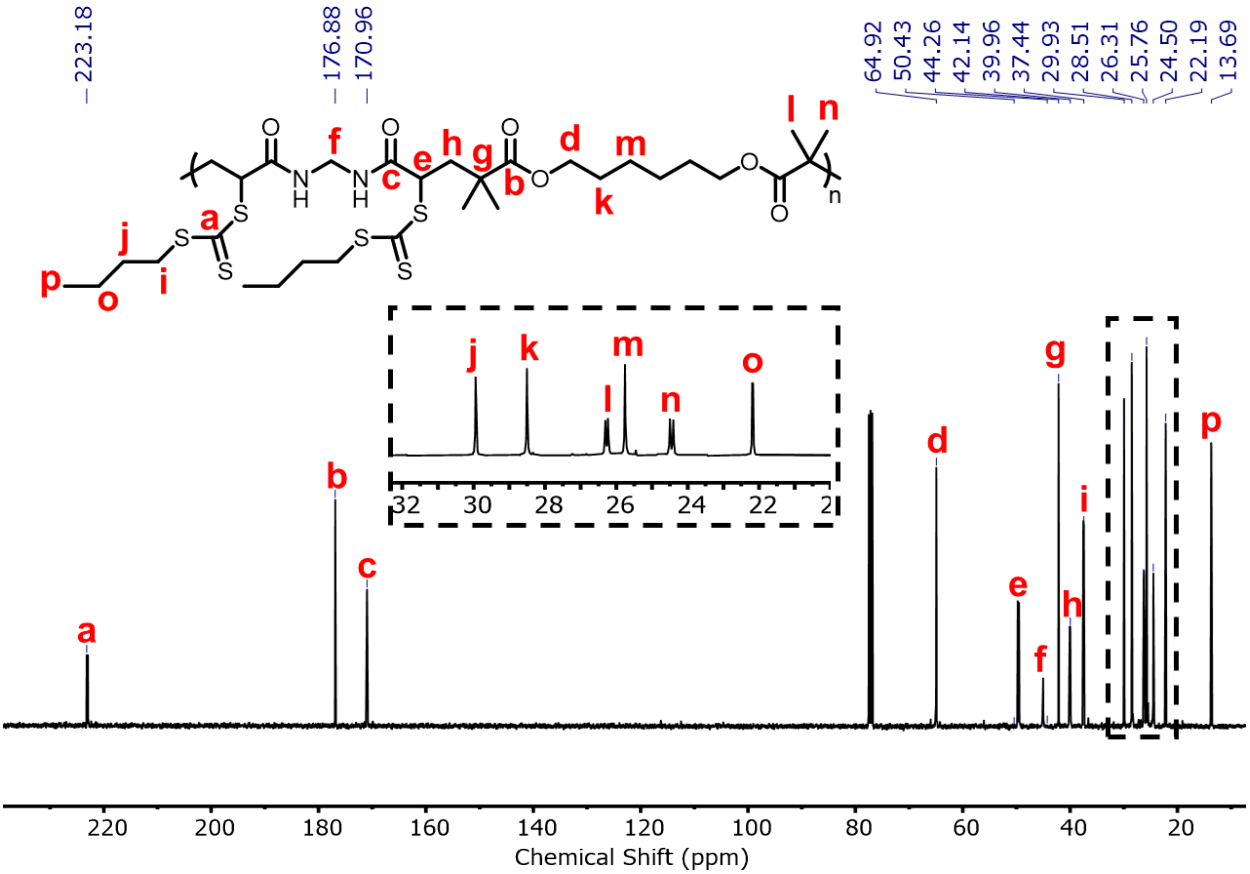

Figure S14. ^{13}C NMR spectrum ($CDCl_3$, 400 MHz, 25 °C) of **P(MBA-*alt*-CTA$_2$)**.

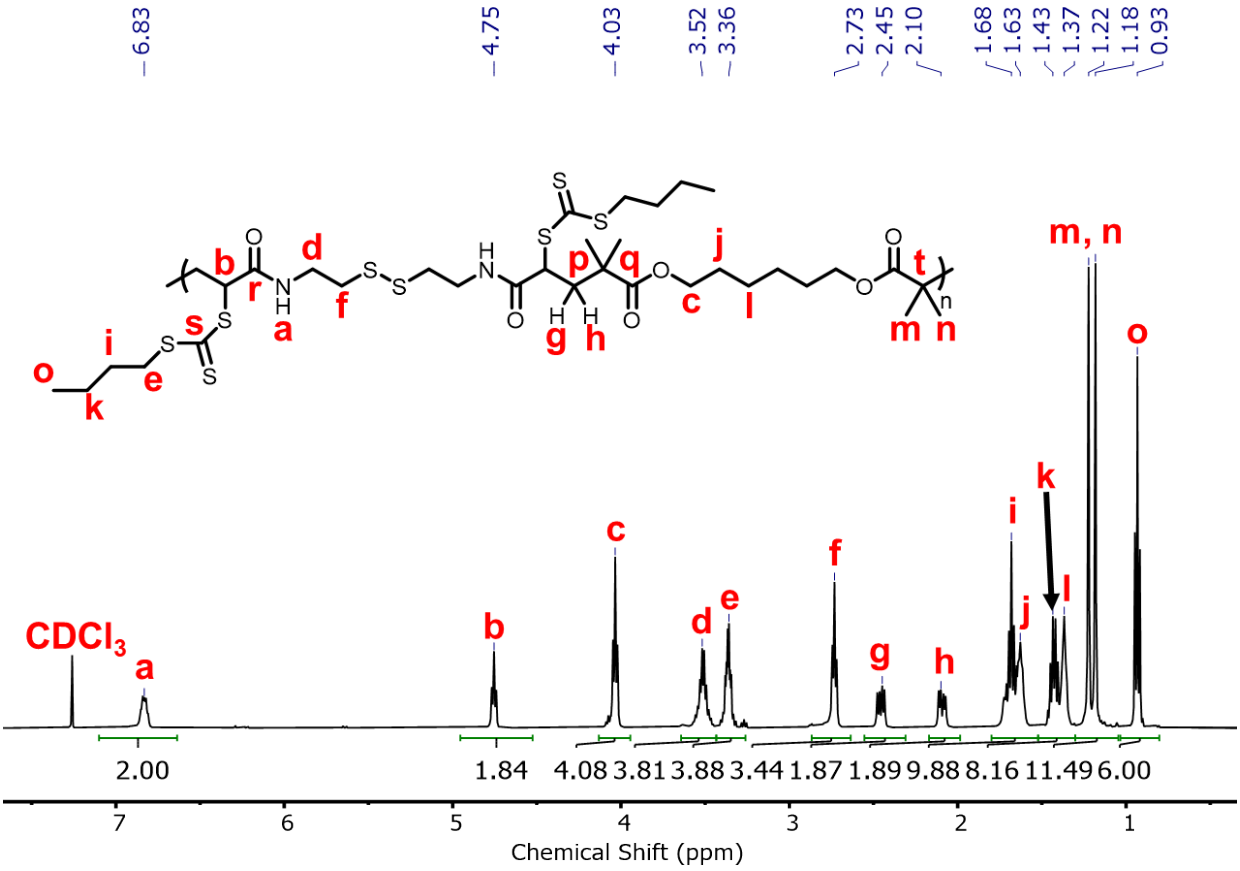

Figure S15. ^{1}H NMR spectrum ($CDCl_3$, 500 MHz, 25 °C) of **P(CBA-*alt*-CTA$_2$).**

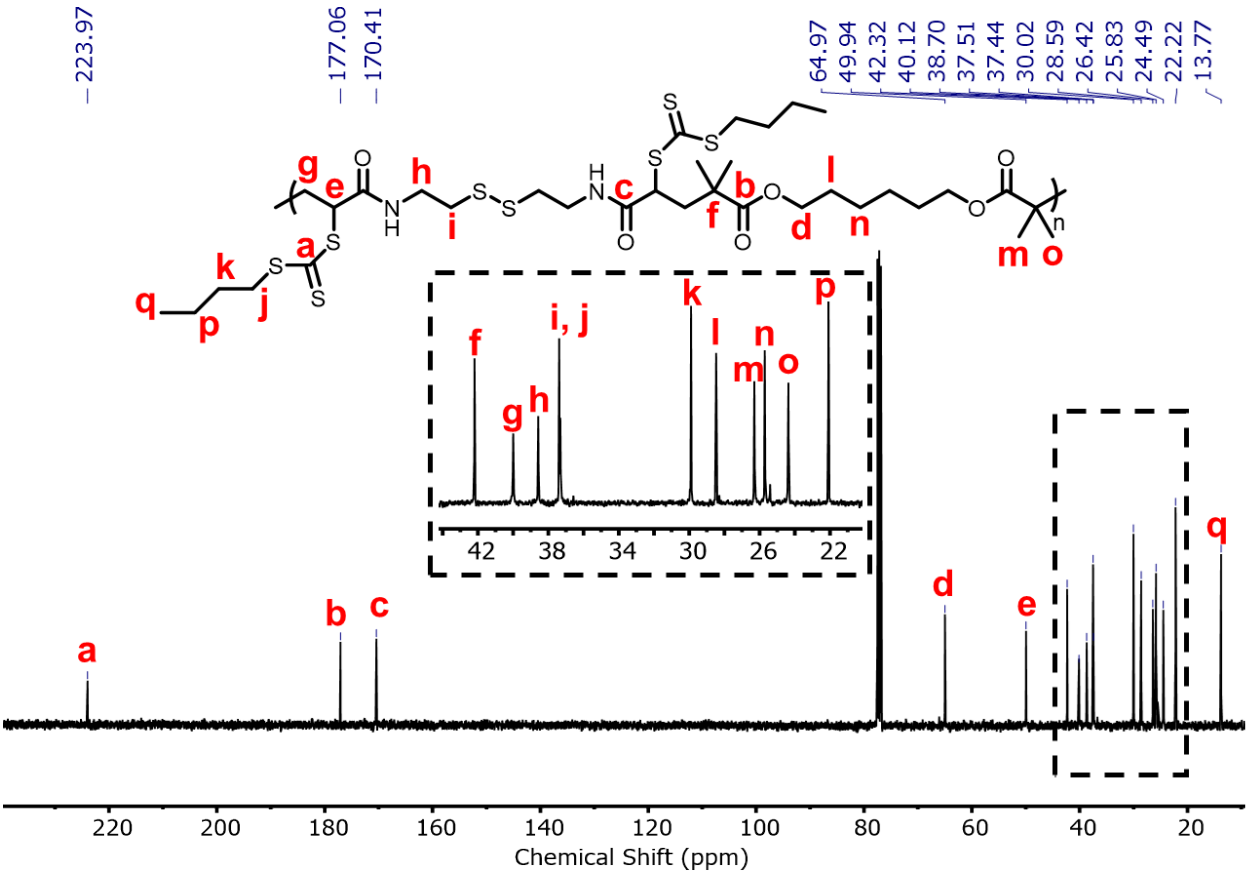

Figure S16. ^{13}C NMR spectrum ($CDCl_3$, 400 MHz, 25 °C) of **P(CBA-*alt*-CTA$_2$)**.

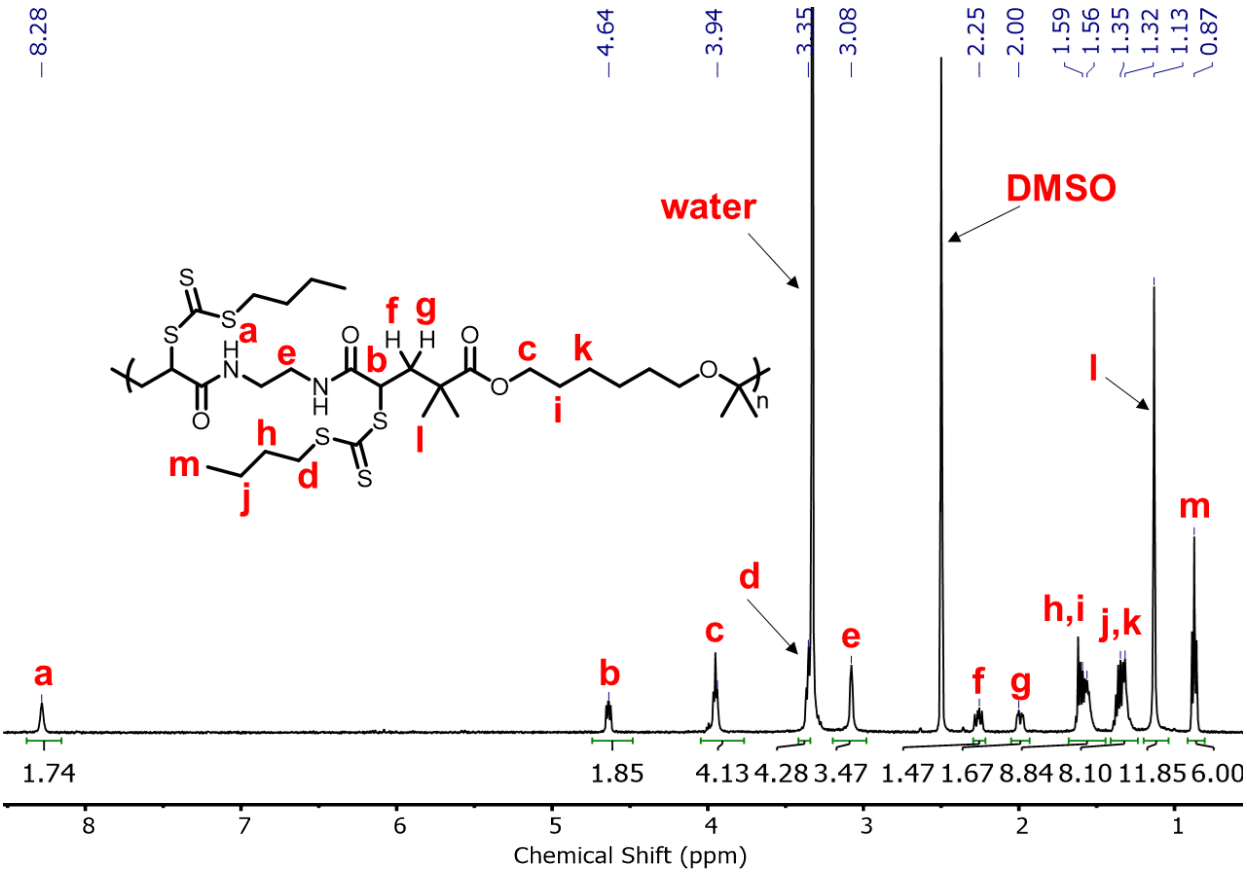

Figure S17. ^{1}H NMR spectrum (DMSO-d_6, 500 MHz, 25 °C) of **P(EBA-*alt*-CTA$_2$)**.

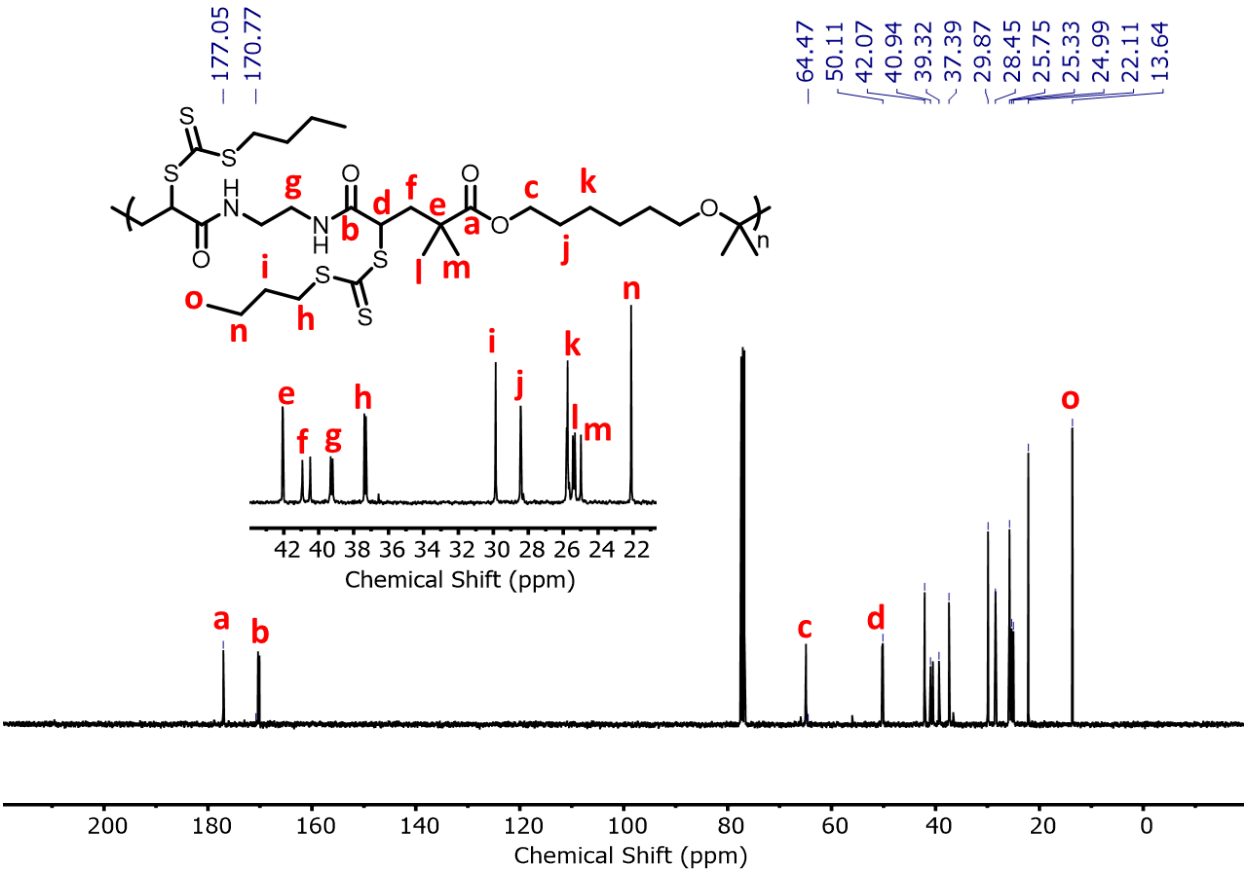

Figure S18. ^{13}C NMR spectrum ($CDCl_3$, 400 MHz, 25 °C) of **P(EBA-*alt*-CTA$_2$).**

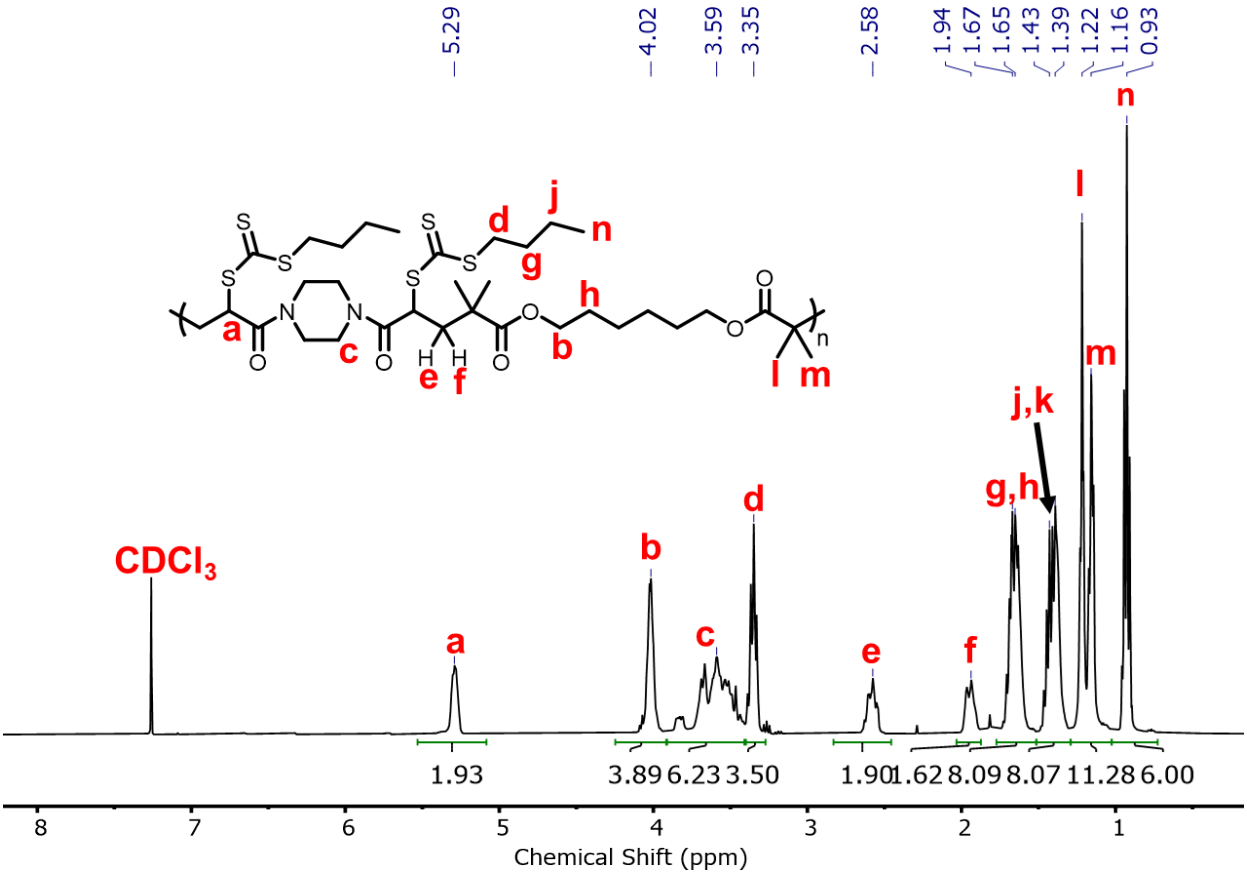

Figure S19. ^{1}H NMR spectrum ($CDCl_3$, 400 MHz, 25 °C) of **P(PBA-*alt*-CTA$_2$)**.

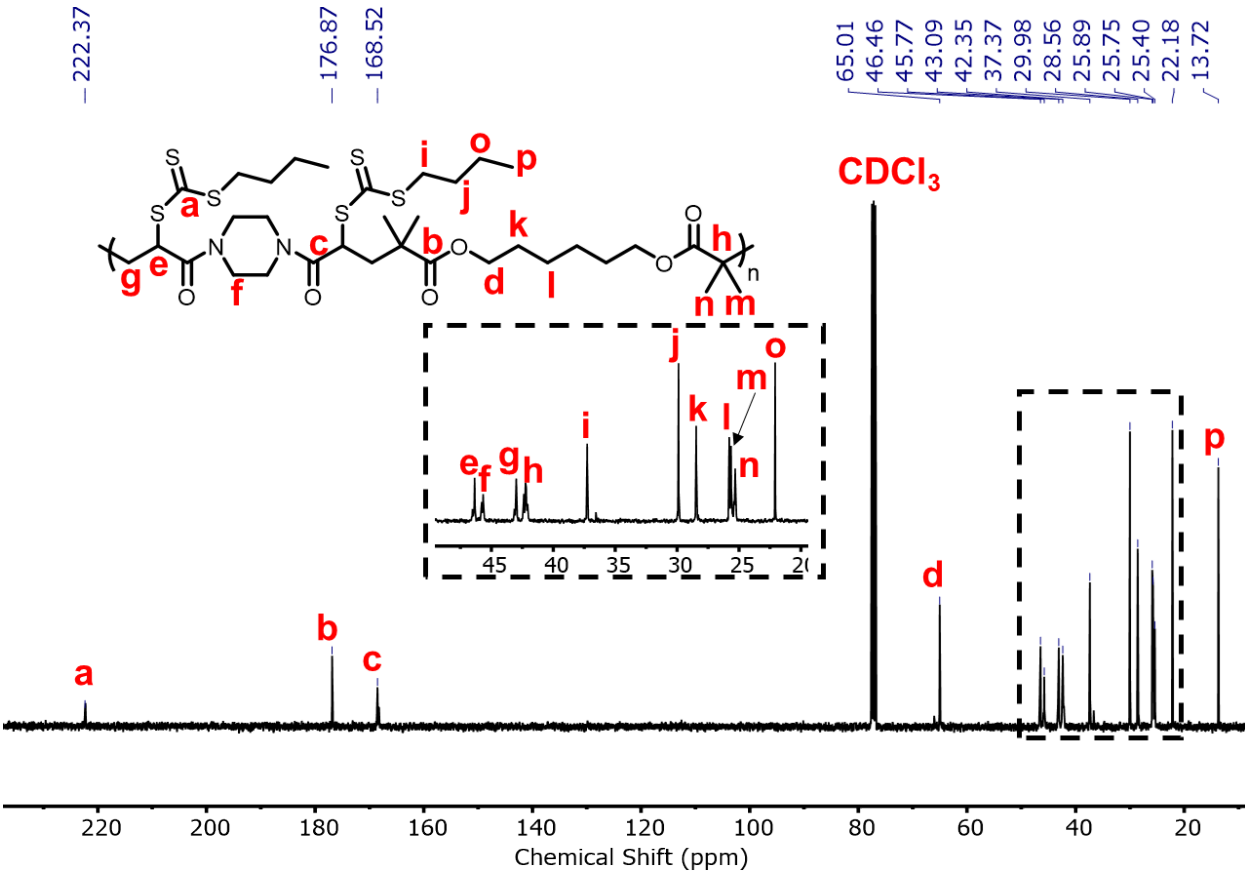

Figure S20. ^{1}H NMR spectrum ($CDCl_3$, 400 MHz, 25 °C) of **P(PBA-*alt*-CTA$_2$)**.

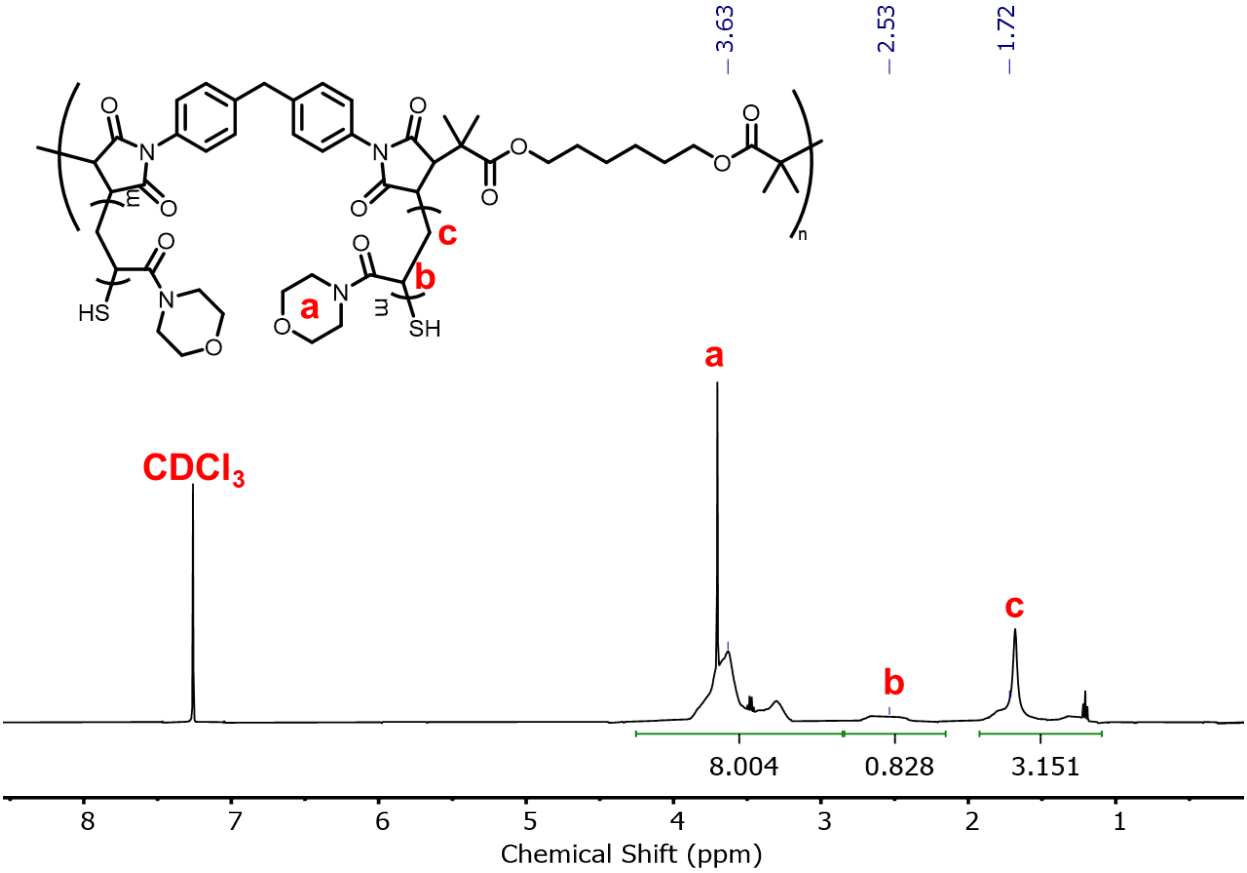

Figure S21. ^{1}H NMR spectrum ($CDCl_3$, 400 MHz, 25 °C) of **PBM-*alt*-CTA$_2$-*graft*-P(NAM)-SH.**

7. Isolated Polymer GPC Chromatograms

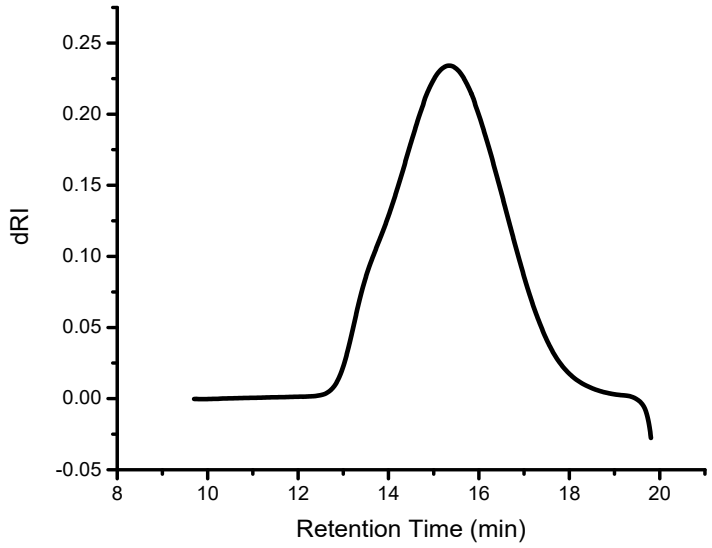

Figure S22. GPC Chromatogram (DMAc, 50 °C, dRI detection) of **P(CBA-*alt*-CTA$_2$)**.

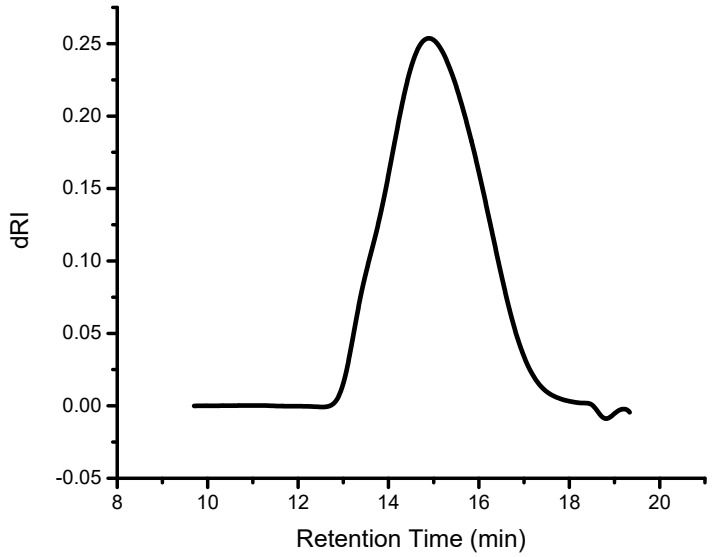

Figure S23. GPC Chromatogram (DMAc, 50 °C, dRI detection) of **P(MBA-*alt*-CTA$_2$)**.

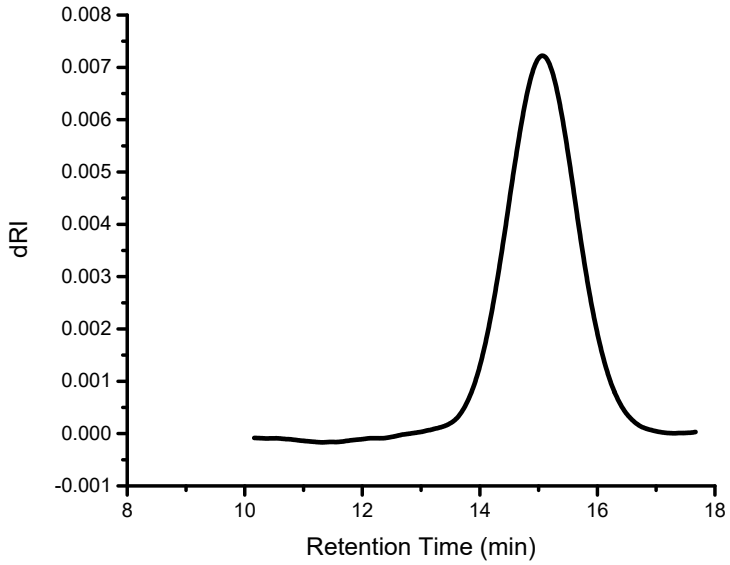

Figure S24. GPC Chromatogram (DMAc, 50 °C, dRI detection) of **P(EBA-*alt*-CTA$_2$)**.

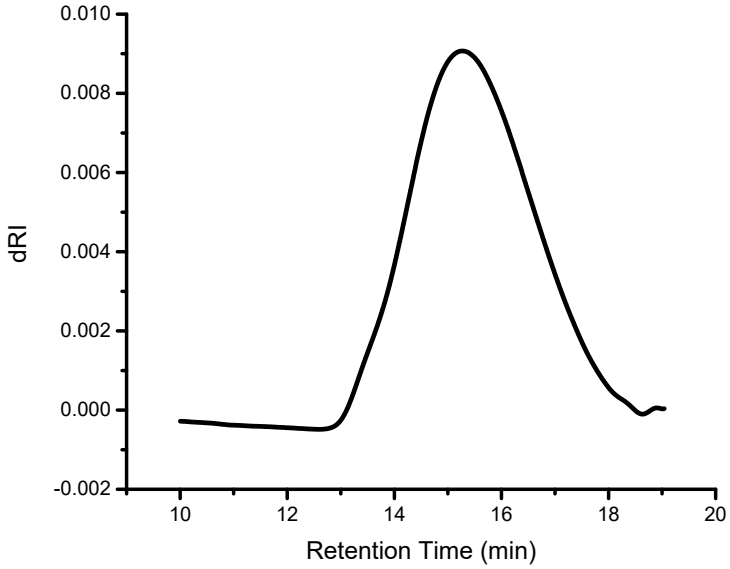

Figure S25. GPC Chromatogram (DMAc, 50 °C, dRI detection) of **P(PBA-*alt*-CTA$_2$)**.

8. DSC Thermograms

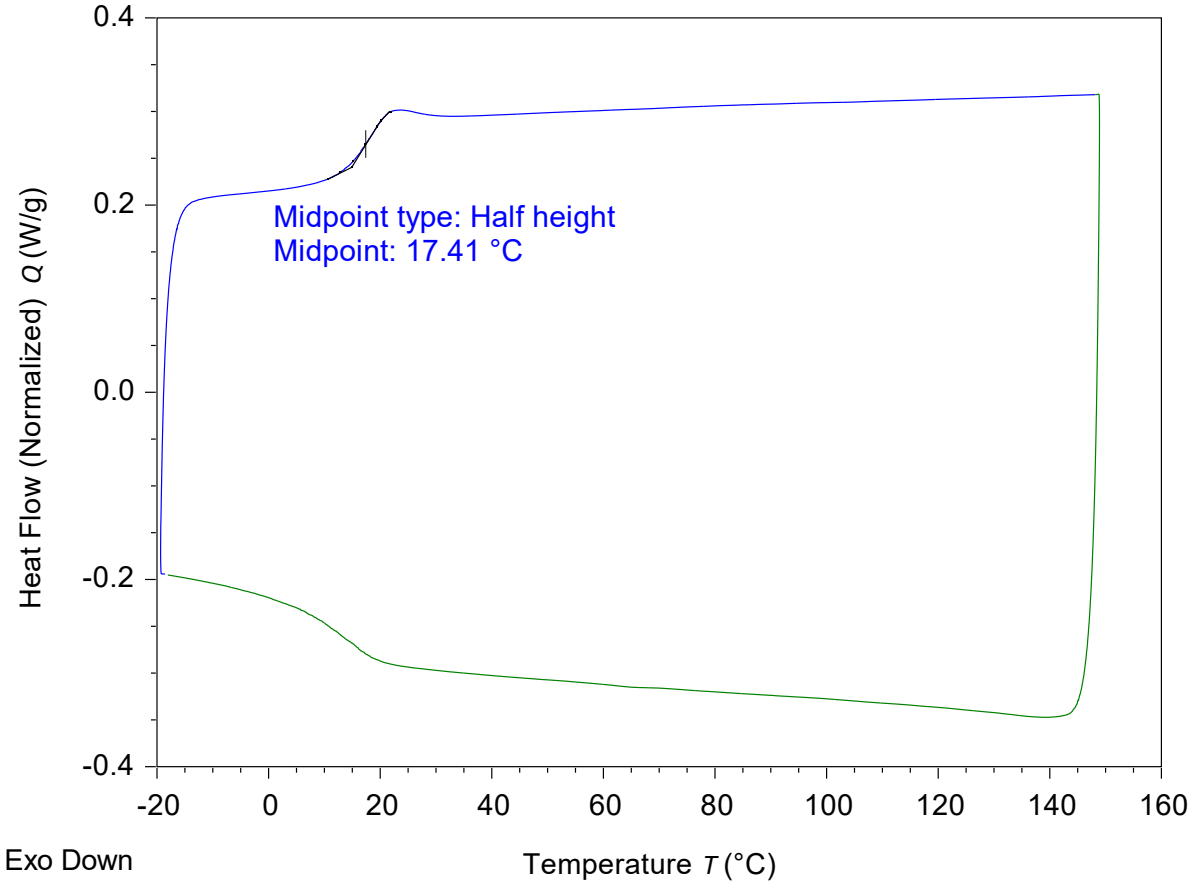

Figure S26. DSC Thermogram of **P(MBA-*alt*-CTA$_2$)**.

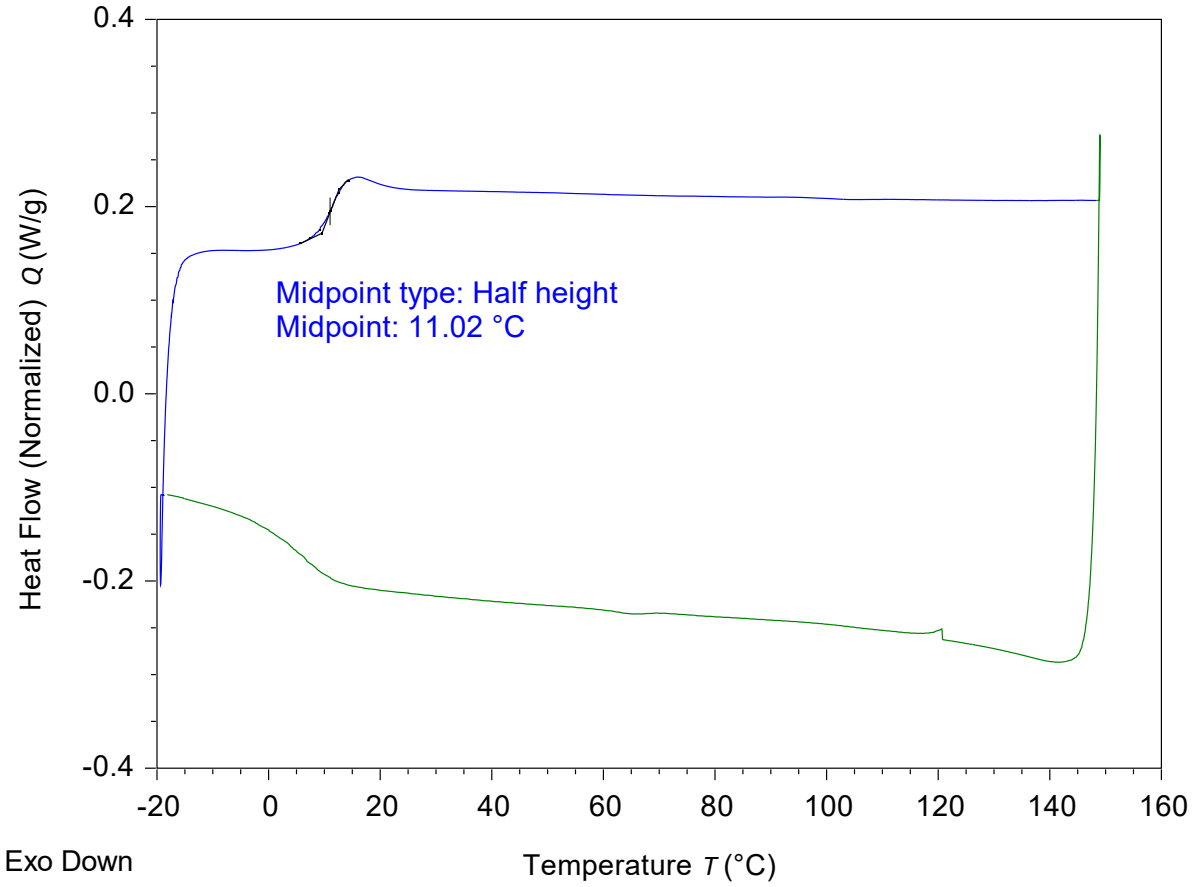

Figure S27. DSC Thermogram of **P(CBA-*alt*-CTA$_2$)**.

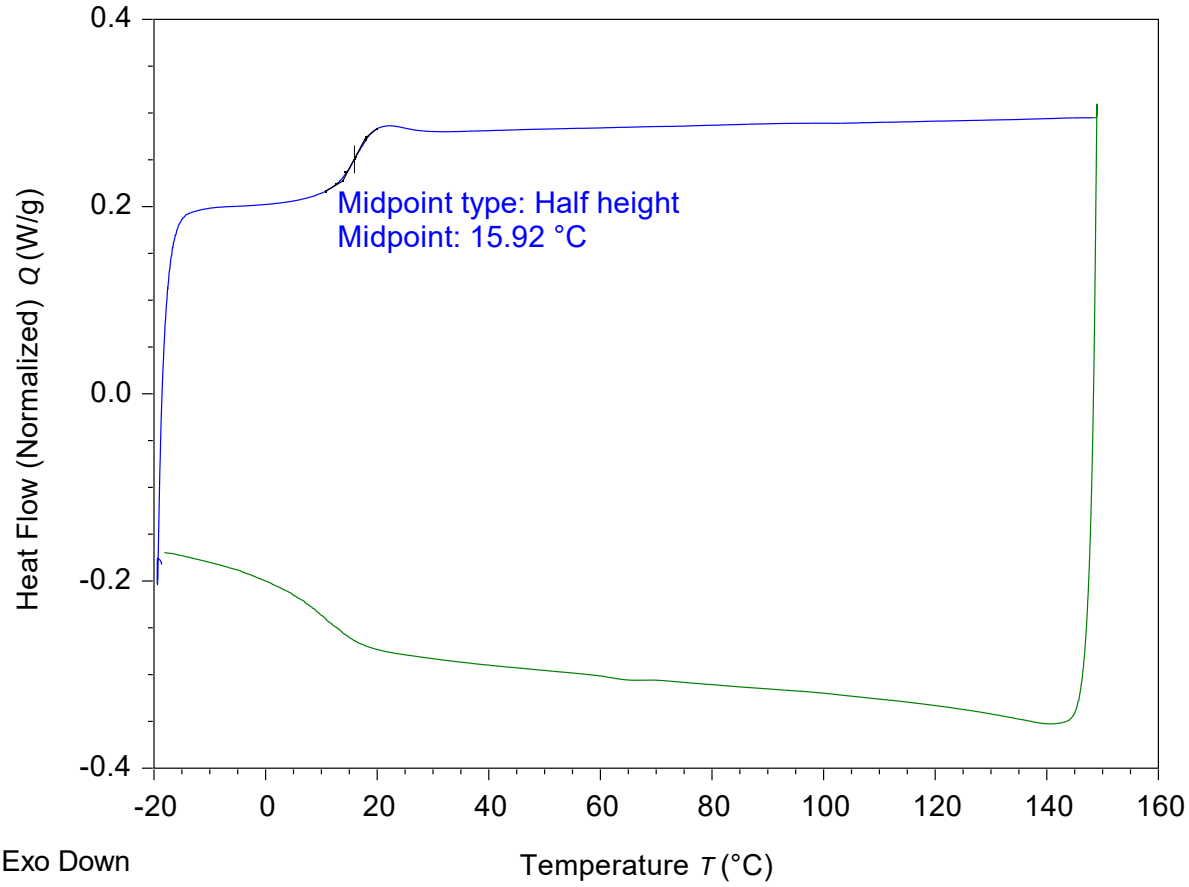

Figure S28. DSC Thermogram of **P(EBA-*alt*-CTA$_2$)**.

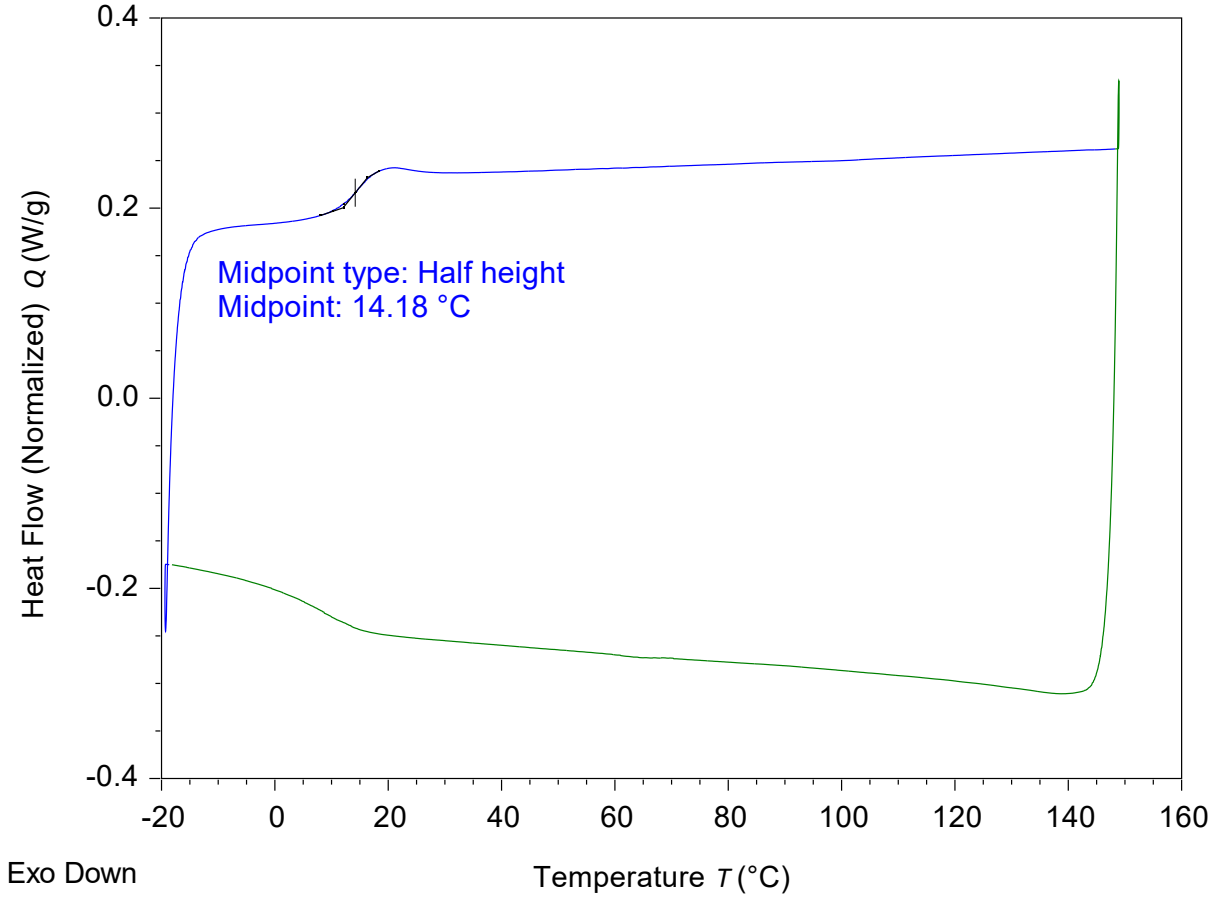

Figure S29. DSC Thermogram of **P(PBA-*alt*-CTA$_2$)**.

9. TGA Thermograms

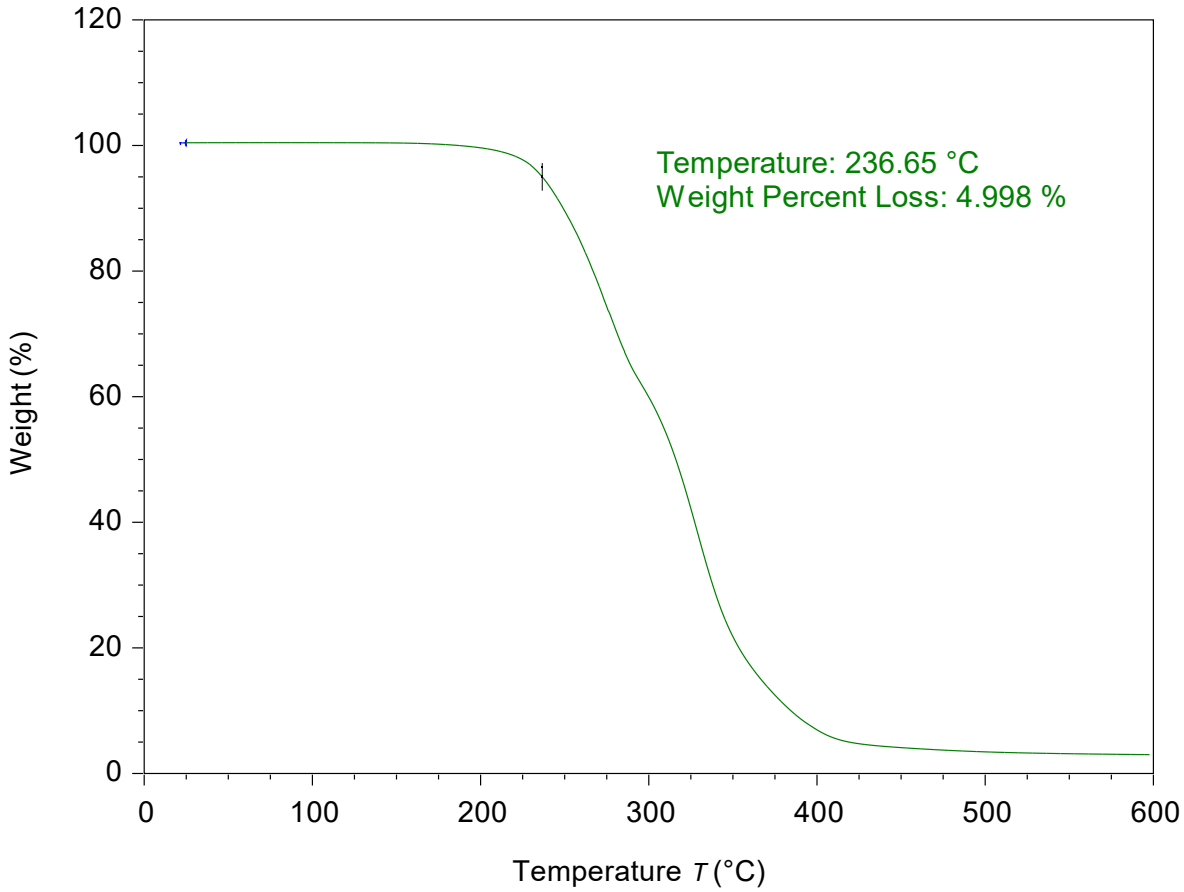

Figure S30. TGA Thermogram of **P(MBA-*alt*-CTA$_2$)**.

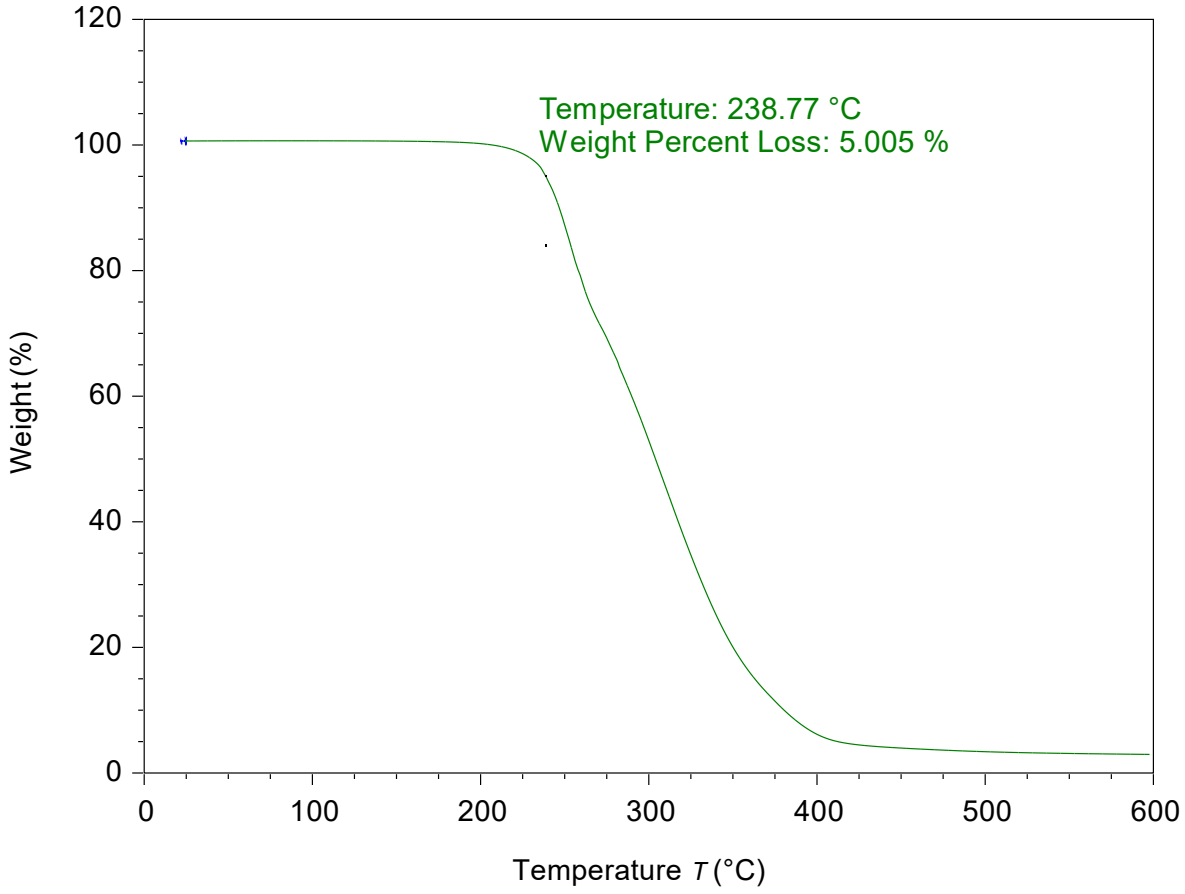

Figure S31. TGA Thermogram of **P(CBA-*alt*-CTA$_2$)**.

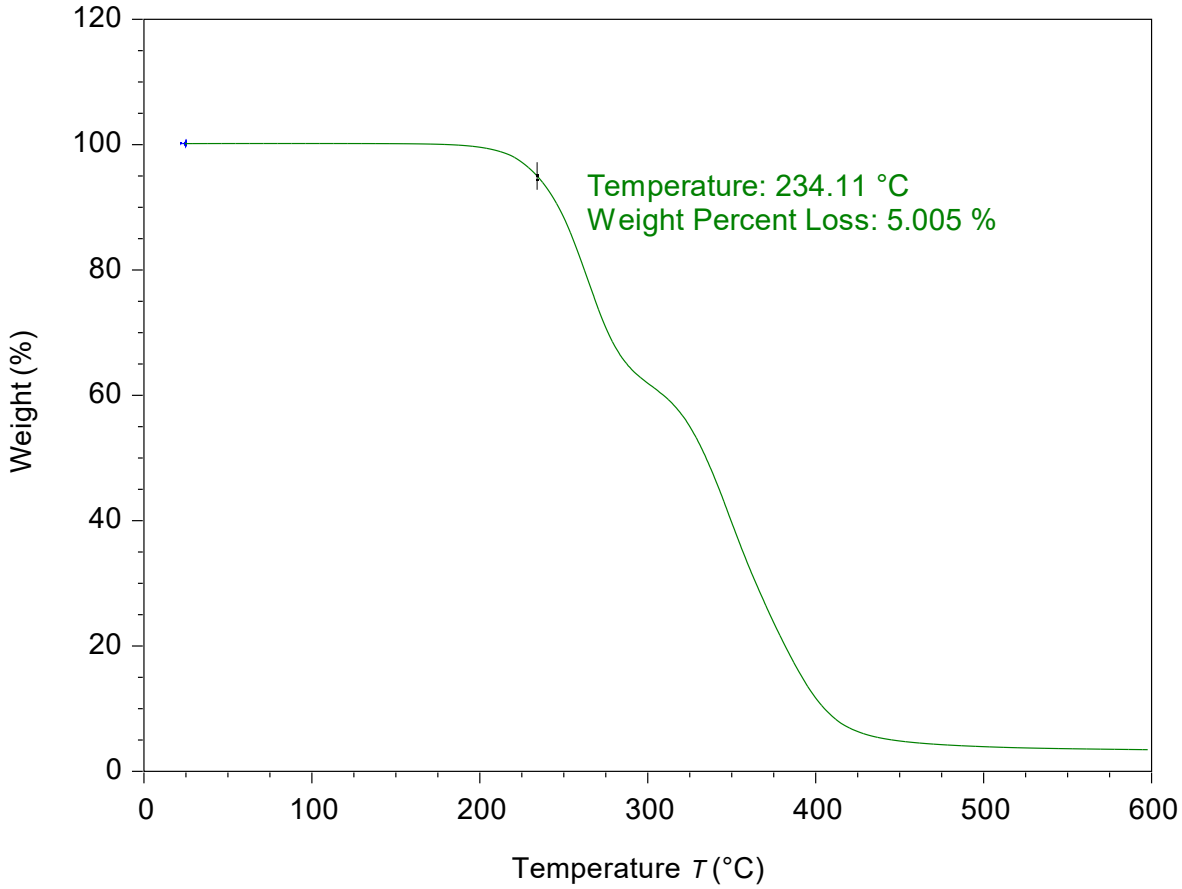

Figure S32. TGA Thermogram of **P(EBA-*alt*-CTA$_2$)**.

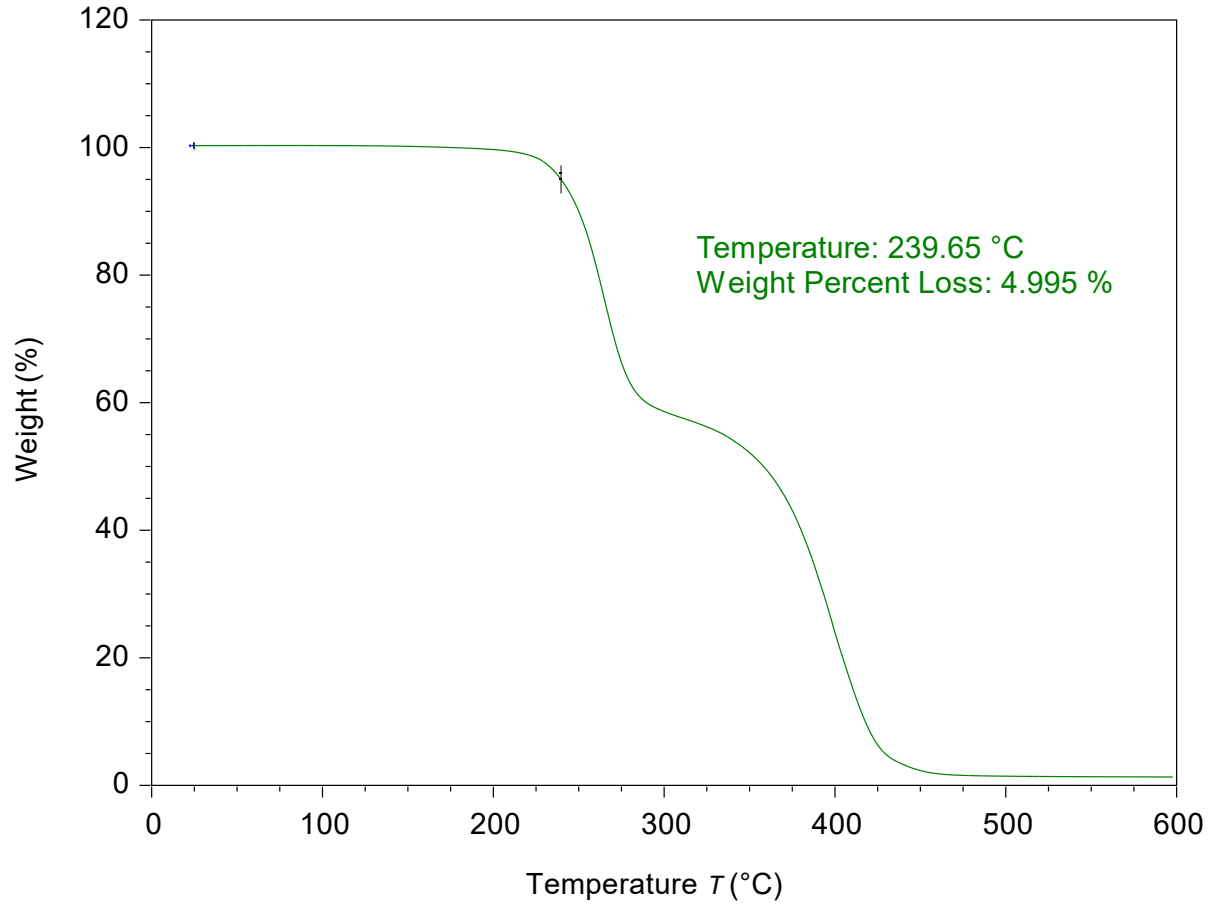

Figure S33. TGA Thermogram of **P(PBA-*alt*-CTA$_2$)**.

10. Triple Detection GPC Chromatograms

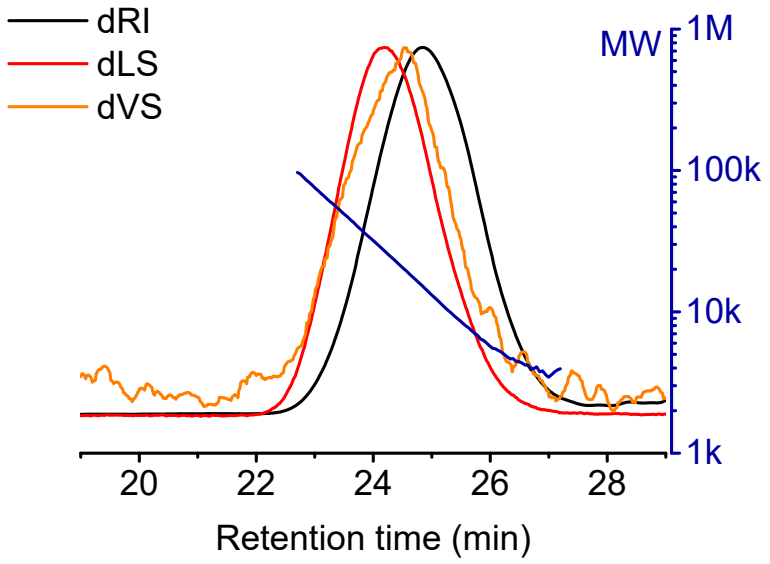

Figure S34. GPC chromatograms (THF, 25 °C, triple detection) of **P(MBA-*alt*-CTA$_2$)** used for producing Mark-Houwink-Sakurada plot.

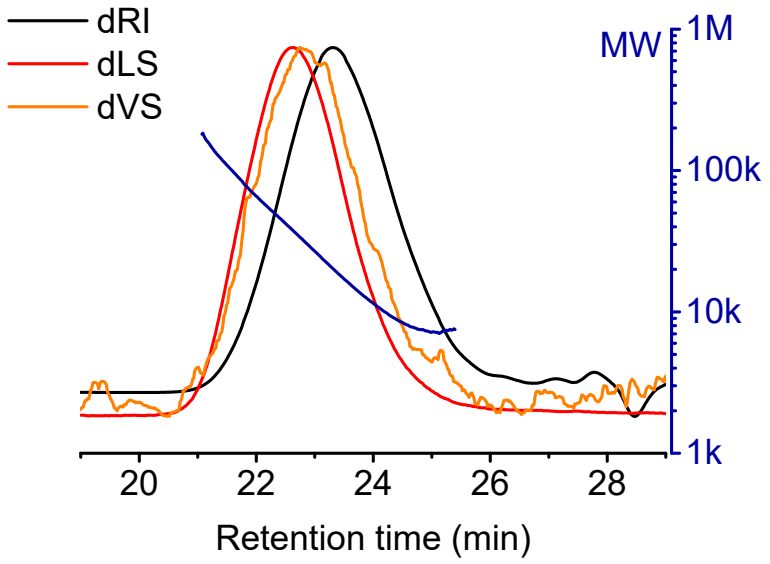

Figure S35. GPC chromatograms (THF, 25 °C, triple detection) of **P(CBA-*alt*-CTA$_2$)** used for producing Mark-Houwink-Sakurada plot.

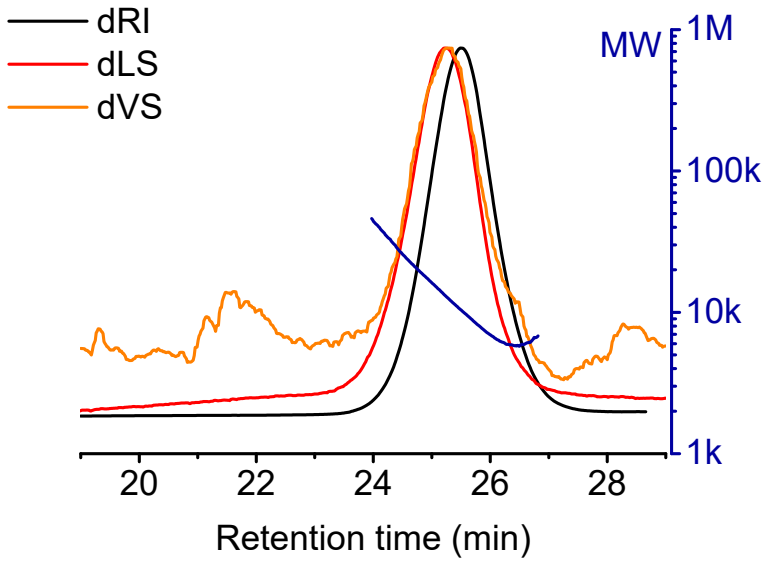

Figure S36. GPC chromatograms (THF, 25 °C, triple detection) of **P(EBA-*alt*-CTA$_2$)** used for producing Mark-Houwink-Sakurada plot.

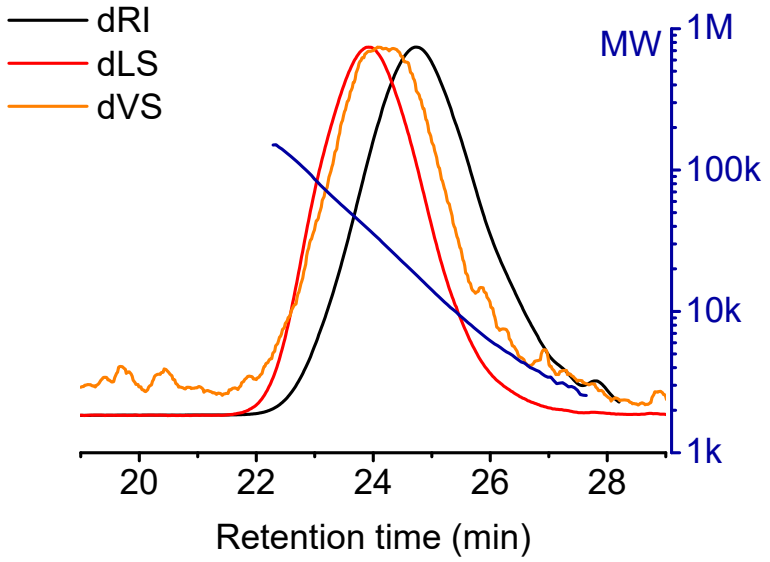

Figure S37. GPC chromatograms (THF, 25 °C, triple detection) of **P(PBA-*alt*-CTA$_2$)** used for producing Mark-Houwink-Sakurada plot.

11. Mark-Houwink-Sakurada Plot

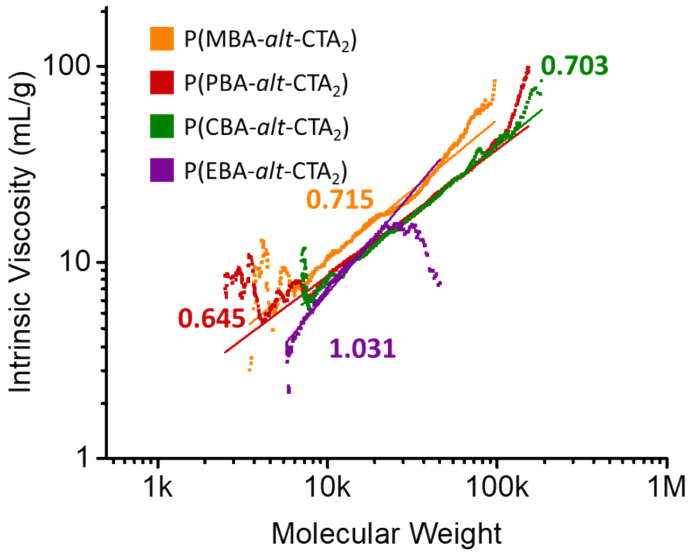

Figure S38. Mark-Houwink-Sakurada plot of the RAFT step-growth polymers as measured by GPC with viscometric detection (THF, 25 °C)

12. Spectra and Chromatogram from Degradation Studies

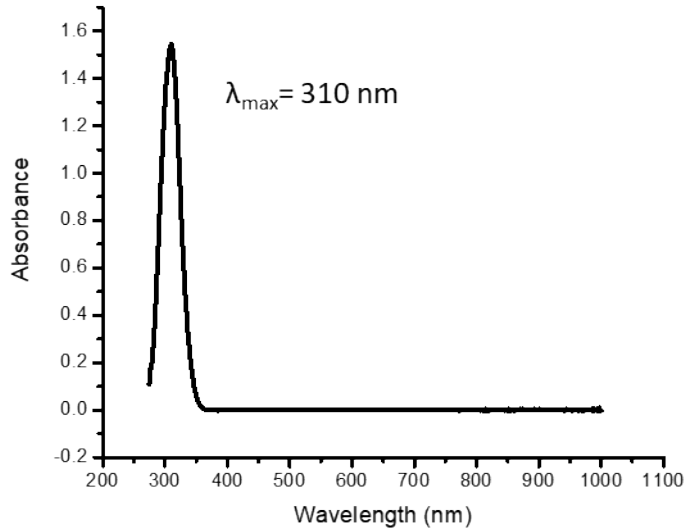

Figure S39. UV-Vis spectra of **P(MBA-*alt*-CTA$_2$)** in DMAc. Note the strong absorbance at 310 nm attributed to the π->π* transition of the pendant trithiocarbonate Z group.

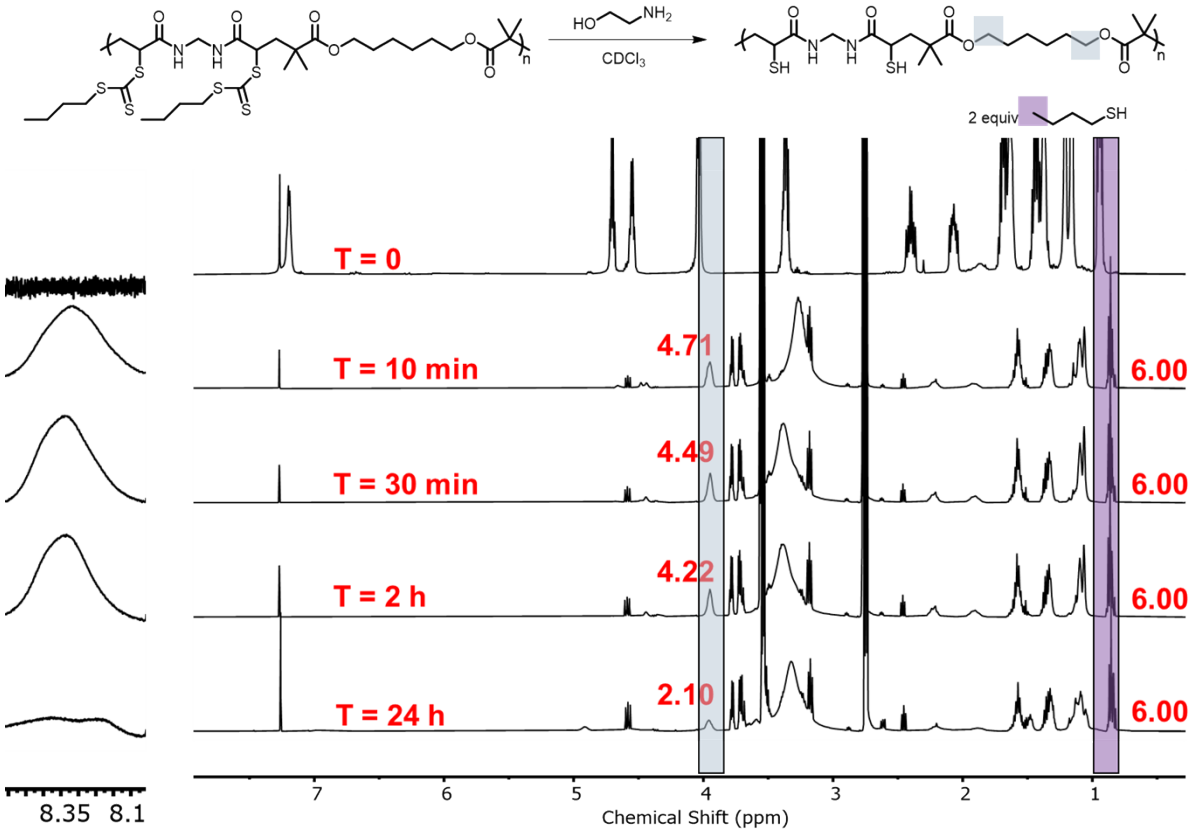

Figure S40. ^{1}H NMR spectra ($CDCl_3$, 400 MHz, 25 °C) before and after the addition of excess ethanolamine to **P(MBA-*alt*-CTA$_2$)**. Note the disappearance of the CH_2 (in blue) adjacent to the ester of the polymer backbone, relative to the CH_3 (of free butanethiol). This indicated ester degradation. **It is important to note that the CH_2 overlaps with the broad resonance of ethanolamine so the exact integral could not be measured.**

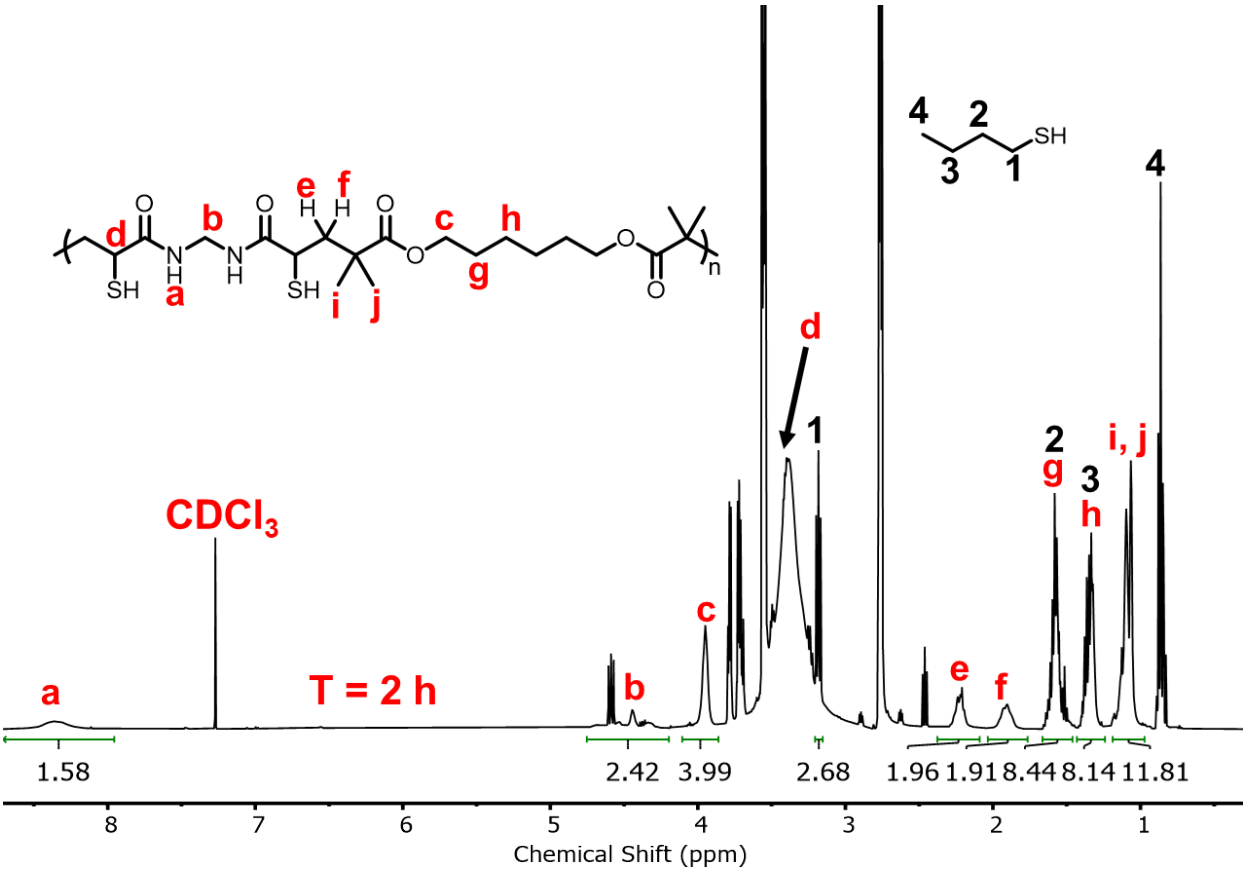

Figure S41. ^{1}H NMR spectra ($CDCl_3$, 400 MHz, 25 °C) 2 h after the addition of excess ethanolamine to **P(MBA-*alt*-CTA$_2$)**. Note the presence of the intermediate **P(MBA-*alt*-CTA$_2$)-SH** the species generated by aminolysis of the trithiocarbonate.

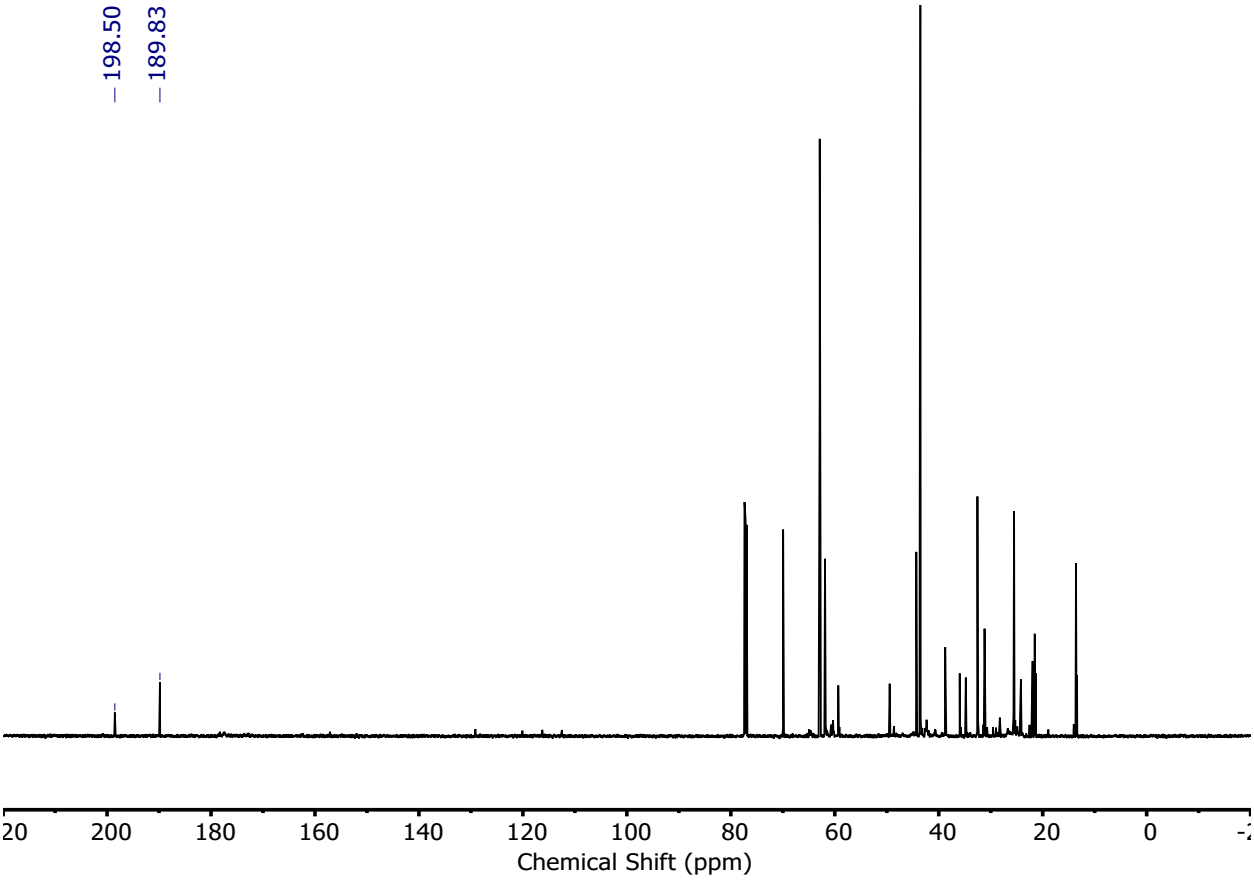

Figure S42. ^{13}C NMR spectra ($CDCl_3$, 400 MHz, 25 °C) 24 h after the addition of excess ethanolamine to **P(MBA-*alt*-CTA$_2$)**. Note the presence of a significantly downfield peak (198.5 ppm) indicative of thiolactone formation.

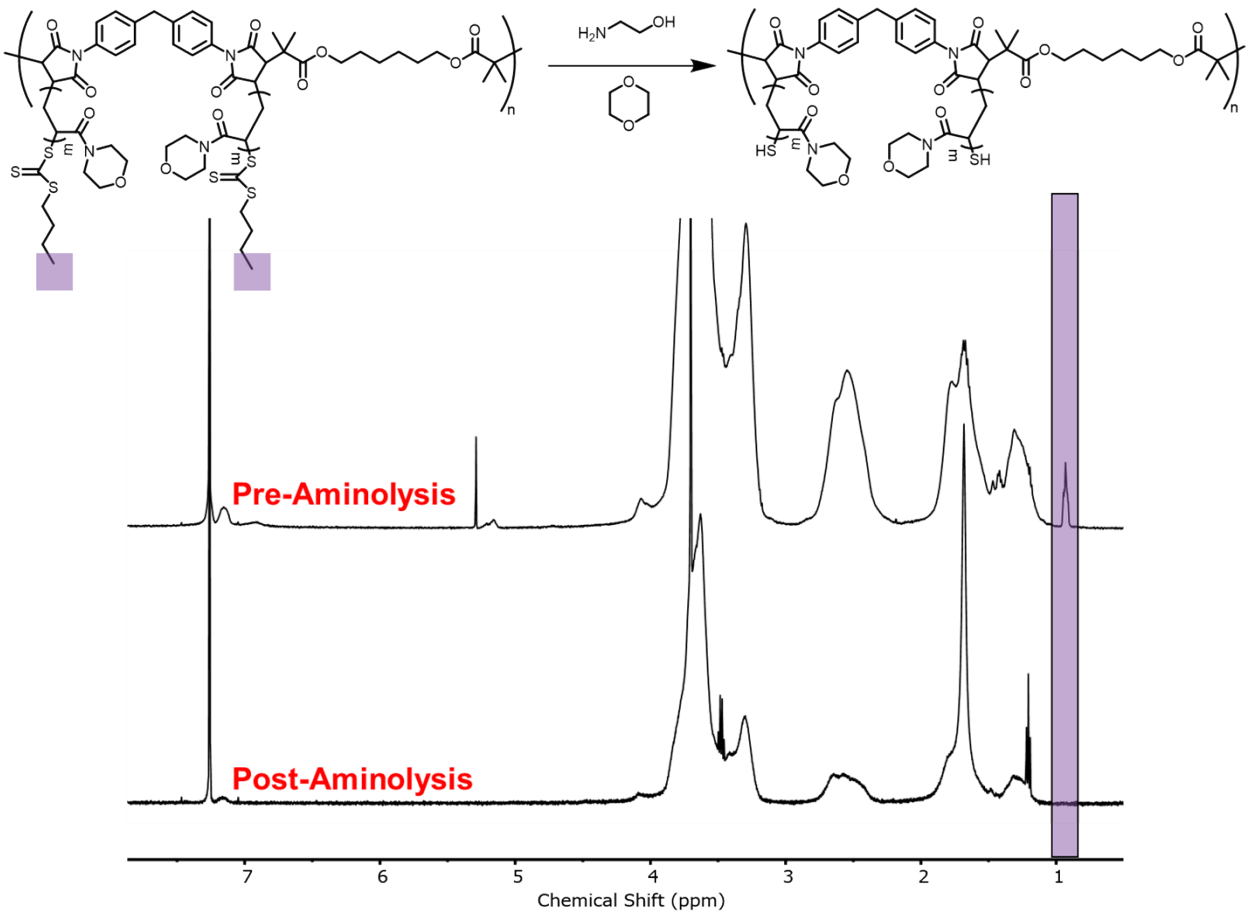

Figure S43. ^{1}H NMR spectra ($CDCl_3$, 400 MHz, 25 °C) of **PBM-*alt*-CTA$_2$-*graft*-P(NAM)** and isolated **PBM-*alt*-CTA$_2$-*graft*-P(NAM)-SH** after aminolysis in dioxane. Note the disappearance of the CH_3 (highlighted in purple) associated with the RAFT Z group indicative of successful Z group removal.

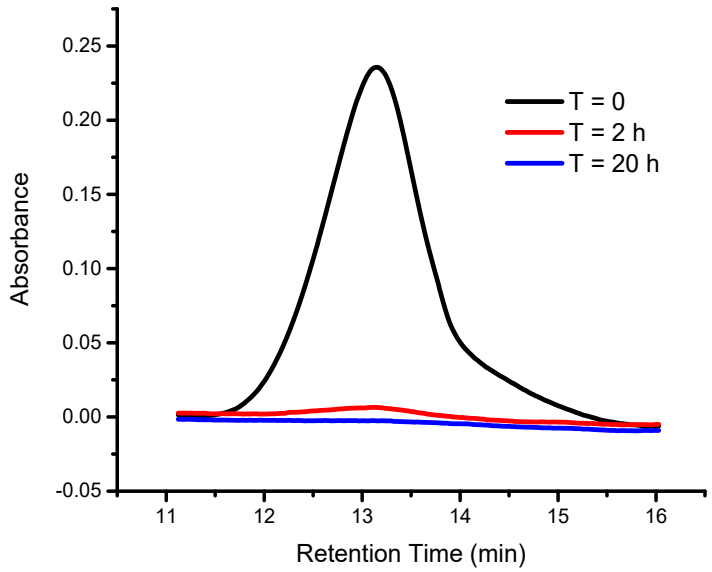

Figure S44. GPC Chromatogram (DMAc, 50°C, UV-Vis detection at 308 nm) **of PBM-*alt*-CTA$_2$-*graft*-P(NAM)** before and after the addition of excess ethanolamine (relative to RAFT end groups).

13. References

1 P. T. Boeck, N. E. Archer, J. Tanaka and W. You, *Polym. Chem.*, 2022, **13**, 2589–2594.

2 P. J. Flory, *J. Am. Chem. Soc.*, 1936, **58**, 1877–1885.

3 J. Tanaka, N. E. Archer, M. J. Grant and W. You, *J. Am. Chem. Soc.*, 2021, **143**, 15918–15923.